Jonni Lohi

Discrete exterior calculus and higher order Whitney forms

Master's Thesis in Information Technology

March 26, 2019

University of Jyväskylä

Faculty of Information Technology

Author: Jonni Lohi

Contact information: jonni.j.lohi@student.jyu.fi

Supervisors: Lauri Kettunen, and Jukka Räbinä

Title: Discrete exterior calculus and higher order Whitney forms

Työn nimi: Diskreetti ulkoinen laskenta ja korkeamman asteen Whitney-muodot

Project: Master's Thesis

Study line: Applied Mathematics and Scientific Computing

Page count: 71+0

Abstract: Partial differential equations describing various phenomena have a natural expression in terms of differential forms. This thesis discusses higher order Whitney forms as approximations for differential forms. We present how they can be used with discrete exterior calculus to discretise and solve partial differential equations formulated with differential forms.

Keywords: discrete exterior calculus, Whitney forms

Suomenkielinen tiivistelmä: Monenlaisia ilmiöitä kuvaavat osittaisdifferentiaaliyhtälöt voidaan esittää luonnollisella tavalla differentiaalimuotojen avulla. Tämä tutkielma käsittelee korkeamman asteen Whitney-muotoja differentiaalimuotojen approksimaatioina. Tutkielmassa esitetään, kuinka niitä voidaan käyttää diskreetin ulkoisen laskennan kanssa differentiaalimuotojen avulla muotoiltujen osittaisdifferentiaaliyhtälöiden diskretisointiin ja ratkaisemiseen.

Avainsanat: diskreetti ulkoinen laskenta, Whitney-muodot

List of Figures

List of Tables

Contents

1 Introduction

The topic of this thesis is discrete exterior calculus and higher order Whitney forms as approximations for differential forms. Many problems in different scientific disciplines lead to partial differential equations for which the solutions cannot be found analytically. Such problems are discretised and solved numerically using a numerical partial differential equation solving method. Well-known examples of these methods are finite element method and finite volume method. The method considered in this thesis is discrete exterior calculus. It suits particularly well for solving wave propagation problems and has applications in different fields of physics, such as electromagnetism, sound propagation, elastic waves, and quantum mechanics (Räbinä et al. 2018).

In discrete exterior calculus, the partial differential equations are represented using differential forms. The problem is discretised by partitioning the domain into small cells which form a mesh. Since differential forms can be integrated over mesh elements of respective dimension, they can be discretised by considering the array of all such integrals as the discrete version of the differential form.

The solution obtained using discrete exterior calculus is a discrete version described above, i.e. we know the integrals over mesh elements. The question arises how to interpolate to get the solution in the usual form. This is where Whitney forms come into play. These geometrical objects are finite elements for differential forms on simplicial meshes (Bossavit 1988). To each mesh element corresponds a Whitney form, and discretising differential forms by integrating over all mesh elements can actually be seen as approximating them in a finite-dimensional space of Whitney forms. Interpolating with these lowest order Whitney forms is simple: the interpolant is a linear combination of all such forms, with the values of the integrals as coefficients.

To increase the accuracy of the solution, one must use a finer mesh, i.e. divide the domain into smaller cells. Another approach is to increase the polynomial degree of the Whitney forms used in approximating differential forms. Whilst using lowest order Whitney forms gives something elementwise linear, with second order Whitney forms we get piecewise

quadratic approximations.

Lowest order Whitney forms as finite elements have been known for a long time (Bossavit 1988). Higher order Whitney forms have been discussed in the literature as well, and their use has been studied with numerical experiments (Rapetti 2007; Bonazzoli and Rapetti 2017; Bonazzoli, Rapetti, and Venturini 2018). However, they have not been used in discrete exterior calculus, and thus it makes sense to ask how this could be done. This is the first research problem of the thesis.

Using higher order finite elements generally leads to more expensive computations, and with lowest order elements a finer mesh could be used at the same computational costs. Therefore, it's logical to study whether higher order Whitney forms are worth using or would it be more efficient to keep using lowest order forms and further refine the mesh instead. This is the second research problem.

Based on the method we developed, Whitney forms are implemented on a DEC-based wave simulation software. Although higher order Whitney forms are discussed in the general case, we only consider the implementation of second order forms. The results given by second order forms are compared with those given by lowest order forms.

Chapter 2 briefly presents some mathematical background needed in building discrete exterior calculus. In Chapter 3 we represent the definition of Whitney forms and show how they can be used to approximate differential forms. In Chapter 4 we give an overview of discrete exterior calculus and discuss a numerical solution of Maxwell's equations as an example. Chapter 5 is the practical part of the thesis; it considers the implementation of the approximations with second order Whitney forms and their application in discrete exterior calculus. The evaluation of the results is also contained in Chapter 5. Chapter 6 concludes the main points of the thesis.

2 Mathematical background

The workspace in discrete exterior calculus is given by the mathematical concept of manifold. Manifolds come with a topological structure by definition, but there are additional structures that enable more things to be done on them. Smooth manifolds admit a smooth structure, which allows one to do calculus on them. Orientable manifolds can be oriented, and Riemannian manifolds come with a metric. These additional structures provide us with the tools needed to do discrete exterior calculus. These tools are presented in this chapter, when we go through some preliminary mathematical concepts.

We define metric tensor and differential forms in Sections 2.1 and 2.2. Then, in Sections 2.3 and 2.4, we present two important operators on differential forms: the exterior derivative and the Hodge star operator. The coverage is brief, and the reader is assumed to have prior knowledge of differential geometry. For more detailed discussion, proofs, and reference, see any textbook about the subject, e.g. Lee (2012), Bishop and Goldberg (1980), Munkres (1991), Abraham, Marsden, and Ratiu (2012), Boothby (1986), or Spivak (1999).

2.1 Metric tensor

Recall that the space of covariant k-tensors on a finite-dimensional vector space V is the space of k-multilinear maps from V onto $\mathbb{R}$ denoted by $T^k(V)$. The tensor product of a covariant k-tensor T and a covariant l-tensor S is a covariant $(k+l)$-tensor denoted by $T \otimes S$ and defined by

$$(T \otimes S)(v_1, \ldots, v_k, v_{k+1}, \ldots, v_{k+l}) = T(v_1, \ldots, v_k) S(v_{k+1}, \ldots, v_{k+l}).$$

Let M be a smooth manifold of dimension n. For each $p \in M$, the tangent space T_pM is an n-dimensional vector space, so we can consider $T^k(T_pM)$, the space of covariant k-tensors on T_pM. The bundle of covariant k-tensors, denoted by T^kTM, is the disjoint union of these spaces for each $p \in M$:

$$T^kTM = \coprod_{p \in M} T^k(T_pM).$$

A covariant k-tensor field on M is then a map from M onto T^kTM whose value at each point $p \in M$ is a covariant k-tensor on T_pM. We denote the space of smooth covariant k-tensor fields on M by $\mathcal{T}^k(M)$. In this thesis, by tensors and tensor fields we always mean covariant tensors and covariant tensor fields, omitting the word "covariant". The tensor product is extended for tensor fields pointwise.

A Riemannian metric on a smooth manifold M is a symmetric smooth 2-tensor field $g \in \mathcal{T}^2(M)$ whose value g_p at each point $p \in M$ is a symmetric positive definite 2-tensor on the tangent space T_pM. A Riemannian manifold (M,g) is a smooth manifold M equipped with a Riemannian metric g.

The requirement of positive definiteness of the metric can be relaxed. A pseudo-Riemannian metric is a symmetric smooth 2-tensor field whose value is nondegenerate at each point: for all $p \in M$ and all nonzero $X \in T_pM$, there exists $Y \in T_pM$ such that $g_p(X,Y) \neq 0$. Discrete exterior calculus could be built using this more general pseudo-Riemannian metric, but for our purposes it suffices to consider Riemannian metrics. Thus, in this thesis by metric or metric tensor we refer to a Riemannian metric on a smooth manifold.

A simple example of a Riemannian manifold is the Euclidean space, i.e. $\mathbb{R}^n$ with the Euclidean metric. The metric tensor can be written in standard Cartesian coordinates as

$$g = \sum_{i=1}^{n} dx_i \otimes dx_i.$$

In Cartesian coordinates, this metric corresponds to the usual inner product of vectors:

$$g(X,Y) = \sum_{i=1}^{n} X_i Y_i.$$

2.2 Differential forms

Recall that a k-tensor ω on a finite-dimensional vector space V is alternating if it changes sign whenever two of its arguments are interchanged: for all $v_1,\dots,v_k \in V$ and $i \neq j$, $\omega(v_1,\dots,v_i,\dots,v_j,\dots,v_k) = -\omega(v_1,\dots,v_j,\dots,v_i,\dots,v_k)$. The vector space of alternating k-tensors on V is denoted by $\Lambda^k(V)$, and it's a subspace of the space of all k-tensors $T^k(V)$.

The alternation operator $\mathrm{Alt} : T^k(V) \to \Lambda^k(V)$ is a projection onto the subspace of alternating

k-tensors, defined by

$$\operatorname{Alt}\omega(v_1,\ldots,v_k)=\frac{1}{k!}\sum_{\sigma\in S_k}(\operatorname{sgn}\sigma)\omega(v_{\sigma(1)},\ldots,v_{\sigma(k)}),$$

where S_k is the group of all permutations of $\{1,\ldots,k\}$. The alternation is a linear operator, and $\operatorname{Alt}\omega=\omega$ if and only if ω is alternating.

The tensor product of alternating tensors is in general not alternating, but there is an operation called wedge product that takes two alternating tensors $\omega\in\Lambda^k(V)$ and $\eta\in\Lambda^l(V)$ and gives an alternating $(k+l)$-tensor, denoted by $\omega\wedge\eta$. Their wedge product is defined as

$$\omega\wedge\eta=\frac{(k+l)!}{k!l!}\operatorname{Alt}(\omega\otimes\eta).$$

The wedge product is bilinear and associative, and when $\omega\in\Lambda^k(V)$ and $\eta\in\Lambda^l(V)$, it satisfies $\omega\wedge\eta=(-1)^{kl}\eta\wedge\omega$.

When $v_1,\ldots,v_n$ is a basis of V and $\varepsilon_1,\ldots,\varepsilon_n$ is the dual basis for V^*, the set

$$\{\varepsilon_{i_1}\wedge\ldots\wedge\varepsilon_{i_k}\,|\,1\le i_1<\ldots<i_k\le n\}$$

forms a basis for $\Lambda^k(V)$. Any element $\omega\in\Lambda^k(V)$ can be written in this basis as

$$\omega=\sum_{i_1<\ldots<i_k}\omega(v_{i_1},\ldots,v_{i_k})\varepsilon_{i_1}\wedge\ldots\wedge\varepsilon_{i_k}.$$

What was explained above can be extended to alternating tensor fields. When M is an n-dimensional smooth manifold, an alternating k-tensor field on M is a tensor field whose value at each point p is an alternating k-tensor on T_pM. Alternating k-tensor fields are called differential k-forms, or simply k-forms, and the vector space of smooth k-forms is denoted by $\Omega^k(M)$. The alternation and the wedge product operations for k-forms are defined pointwise, and any element $\omega\in\Omega^k(M)$ can be written in local coordinates as

$$\omega=\sum_{i_1<\ldots<i_k}\omega_{i_1\ldots i_k}dx_{i_1}\wedge\ldots\wedge dx_{i_k},\tag{2.1}$$

where $\omega_{i_1\ldots i_k}=\omega(\frac{\partial}{\partial x_{i_1}},\ldots,\frac{\partial}{\partial x_{i_k}})$ is a smooth function in the coordinate neighbourhood.

Note that $\Omega^0(M)$ equals the space of smooth functions on M and $\Omega^1(M)$ equals the space of smooth covector fields on M. If $k>n$, then $\Omega^k(M)$ is the zero-dimensional space.

2.3 Exterior derivative and Stokes' theorem

An important operator for differential forms is the exterior derivative, which extends the differential of functions to forms. For each k, the exterior derivative d is the unique $\mathbb{R}$-linear operator $\mathrm{d} : \Omega^k(M) \to \Omega^{k+1}(M)$ satisfying the following properties:

i For $f \in \Omega^0(M)$, $\mathrm{d}f = df$, the usual differential of a smooth function on M.
ii For $\omega \in \Omega^k(M)$ and $\eta \in \Omega^l(M)$, $\mathrm{d}(\omega \wedge \eta) = \mathrm{d}\omega \wedge \eta + (-1)^k \omega \wedge \mathrm{d}\eta$.
iii $\mathrm{d} \circ \mathrm{d} = 0$.

The exterior derivative of a k-form ω can be computed in local coordinates using linearity and (2.1) with the formula

$$\mathrm{d}(\omega_{i_1 \ldots i_k} dx_{i_1} \wedge \ldots \wedge dx_{i_k}) = d\omega_{i_1 \ldots i_k} \wedge dx_{i_1} \wedge \ldots \wedge dx_{i_k}.$$

Differential n-forms can be integrated over oriented n-dimensional smooth manifolds. Although we don't show how integration on manifolds is done, we state the following important result, Stokes' theorem, which holds for the exterior derivative.

Theorem 1 (Stokes' theorem) *Let M be an oriented smooth manifold of dimension n and $\omega \in \Omega^{n-1}(M)$ compactly supported. Then*

$$\int_M \mathrm{d}\omega = \int_{\partial M} \omega.$$

Stokes' theorem generalises the fundamental theorem of calculus and is the basis of discrete exterior calculus.

2.4 Hodge star operator

The goal of this section is to define the Hodge star operator, a canonical isomorphism that takes k-forms to $(n-k)$-forms. For this we use the Riemannian volume form on an oriented Riemannian manifold. For background information of orientations and for more detail about the Riemannian volume form, see Chapter 15 in Lee (2012).

We start by defining flat and sharp operators. Let (M, g) be an oriented Riemannian manifold of positive dimension n. The metric g induces an isomorphism $\flat$ between tangent vectors and

covectors by setting

$$(\flat X)(Y) = g_p(X,Y)$$

for $X, Y \in T_pM$. This operator is called flat and denoted by $\flat$. Its inverse is called sharp and denoted by $\sharp$.

Since M is oriented, there is a unique smooth nonvanishing n-form $dV_g \in \Omega^n(M)$ that satisfies $dV_g(E_1,\ldots,E_n) = 1$ for any local positively oriented orthonormal frame $E_1,\ldots,E_n$. dV_g is called the Riemannian volume form, and in local positively oriented coordinates it can be written as

$$dV_g = \sqrt{\det G}\, dx_1 \wedge \ldots \wedge dx_n,$$

where G is the matrix consisting of elements $g_{ij} = g(\frac{\partial}{\partial x_i}, \frac{\partial}{\partial x_j})$. For $k = 0$, the Hodge star of $f \in \Omega^0(M)$ is defined as $\star f = f dV_g$.

To define the Hodge star for $k \in \{1,\ldots,n\}$, we point out that for each $p \in M$, the metric g determines a unique inner product $\langle \cdot, \cdot \rangle$ on $\Lambda^k(T_pM)$ such that whenever $\omega_1,\ldots,\omega_k,\eta_1,\ldots,\eta_k$ are covectors at p,

$$\langle \omega_1 \wedge \ldots \wedge \omega_k, \eta_1 \wedge \ldots \wedge \eta_k \rangle = \det A,$$

where A is the matrix consisting of elements $A_{ij} = g_p(\sharp\omega_i, \sharp\eta_j)$. Using this inner product, we define the Hodge star operator $\star : \Omega^k(M) \to \Omega^{n-k}(M)$ as the unique linear isomorphism satisfying

$$\omega \wedge \star\eta = \langle \omega, \eta \rangle dV_g \quad \forall \omega, \eta \in \Omega^k(M).$$

When η is the operand of the Hodge star, the image $\star\eta$ is called the Hodge dual of η, sometimes simply the dual of η.

The exterior derivative and the Hodge star operator are of most importance when building discrete exterior calculus because with flat and sharp they enable us to express partial differential operators from vector calculus using differential forms. We end this chapter with an example illustrating this and some of the other things presented thus far.

Example Let $M = \mathbb{R}^3$ with Euclidean metric and standard orientation. Recall that 0-forms are smooth functions. Applying (2.1) in standard Cartesian coordinates, 1-form ω, 2-form η, and 3-form σ can be written as

$$\begin{aligned}\omega &= \omega_1 dx_1 + \omega_2 dx_2 + \omega_3 dx_3,\\ \eta &= \eta_{12} dx_1 \wedge dx_2 + \eta_{13} dx_1 \wedge dx_3 + \eta_{23} dx_2 \wedge dx_3,\\ \sigma &= \sigma_{123} dx_1 \wedge dx_2 \wedge dx_3.\end{aligned}$$

The Hodge duals are given by

$$\begin{aligned}&\star dx_1 = dx_2 \wedge dx_3, && \star(dx_1 \wedge dx_2) = dx_3, && \star(dx_1 \wedge dx_2 \wedge dx_3) = 1,\\ &\star dx_2 = -dx_1 \wedge dx_3, && \star(dx_1 \wedge dx_3) = -dx_2, && \star 1 = dx_1 \wedge dx_2 \wedge dx_3.\\ &\star dx_3 = dx_1 \wedge dx_2, && \star(dx_2 \wedge dx_3) = dx_1, &&\end{aligned}$$

In three dimensions $\star\star = \mathrm{id}$, so the Hodge star operator enables us to identify 0-forms with 3-forms and 1-forms with 2-forms. This actually means that differential forms can be identified with scalar and vector fields. These are called proxy fields and given as follows. A 0-form is already a scalar field, and with the 3-form f we identify the scalar field $\star f$. The corresponding vector field to the 1-form ω is $\sharp\omega$, so with the 2-form η we can identify the vector field $\sharp\star\eta$.

Using the correspondence between differential forms and their proxies, we can now present the vector calculus operators gradient, curl, divergence, and laplacian in terms of differential forms. When f is a smooth function and $F = (F_1, F_2, F_3)$ is a smooth vector field, we have:

i $\nabla f = \sharp \mathrm{d} f$,
ii $\nabla \times F = \sharp\star \mathrm{d} \flat F$,
iii $\nabla \cdot F = \star \mathrm{d} \star \flat F$,
iv $\Delta f = \star \mathrm{d} \star \mathrm{d} f$.

Proof. i: For 0-forms the exterior derivative is just the usual differential of a smooth function, and thus $\sharp \mathrm{d} f = \sharp df = \sharp(\frac{\partial f}{\partial x_1} dx_1 + \frac{\partial f}{\partial x_2} dx_2 + \frac{\partial f}{\partial x_3} dx_3) = (\frac{\partial f}{\partial x_1}, \frac{\partial f}{\partial x_2}, \frac{\partial f}{\partial x_3}) = \nabla f$.

ii:

$$\begin{aligned}
&\sharp\star \mathrm{d}\flat F = \sharp\star \mathrm{d}(F_1 dx_1 + F_2 dx_2 + F_3 dx_3) = \sharp\star(dF_1 \wedge dx_1 + dF_2 \wedge dx_2 + dF_3 \wedge dx_3) \\
&= \sharp\star\left[\left(\frac{\partial F_1}{\partial x_1}dx_1 + \frac{\partial F_1}{\partial x_2}dx_2 + \frac{\partial F_1}{\partial x_3}dx_3\right)\wedge dx_1 + \left(\frac{\partial F_2}{\partial x_1}dx_1 + \frac{\partial F_2}{\partial x_2}dx_2 + \frac{\partial F_2}{\partial x_3}dx_3\right)\wedge dx_2\right. \\
&\quad \left. + \left(\frac{\partial F_3}{\partial x_1}dx_1 + \frac{\partial F_3}{\partial x_2}dx_2 + \frac{\partial F_3}{\partial x_3}dx_3\right)\wedge dx_3\right] \\
&= \sharp\star\left[\frac{\partial F_1}{\partial x_2}dx_2\wedge dx_1 + \frac{\partial F_1}{\partial x_3}dx_3\wedge dx_1 + \frac{\partial F_2}{\partial x_1}dx_1\wedge dx_2 + \frac{\partial F_2}{\partial x_3}dx_3\wedge dx_2\right. \\
&\quad \left. + \frac{\partial F_3}{\partial x_1}dx_1\wedge dx_3 + \frac{\partial F_3}{\partial x_2}dx_2\wedge dx_3\right] \\
&= \sharp\star\left[\left(\frac{\partial F_2}{\partial x_1} - \frac{\partial F_1}{\partial x_2}\right)dx_1\wedge dx_2 + \left(\frac{\partial F_3}{\partial x_1} - \frac{\partial F_1}{\partial x_3}\right)dx_1\wedge dx_3 + \left(\frac{\partial F_3}{\partial x_2} - \frac{\partial F_2}{\partial x_3}\right)dx_2\wedge dx_3\right] \\
&= \sharp\left[\left(\frac{\partial F_2}{\partial x_1} - \frac{\partial F_1}{\partial x_2}\right)dx_3 - \left(\frac{\partial F_3}{\partial x_1} - \frac{\partial F_1}{\partial x_3}\right)dx_2 + \left(\frac{\partial F_3}{\partial x_2} - \frac{\partial F_2}{\partial x_3}\right)dx_1\right] \\
&= \left(\frac{\partial F_3}{\partial x_2} - \frac{\partial F_2}{\partial x_3}, \frac{\partial F_1}{\partial x_3} - \frac{\partial F_3}{\partial x_1}, \frac{\partial F_2}{\partial x_1} - \frac{\partial F_1}{\partial x_2}\right) = \nabla \times F.
\end{aligned}$$

iii:

$$\begin{aligned}
&\star \mathrm{d}\star\flat F = \star \mathrm{d}\star(F_1 dx_1 + F_2 dx_2 + F_3 dx_3) = \star \mathrm{d}(F_1 dx_2\wedge dx_3 - F_2 dx_1\wedge dx_3 + F_3 dx_1\wedge dx_2) \\
&= \star(dF_1\wedge dx_2\wedge dx_3 - dF_2\wedge dx_1\wedge dx_3 + dF_3\wedge dx_1\wedge dx_2) \\
&= \star\left[\left(\frac{\partial F_1}{\partial x_1}dx_1 + \frac{\partial F_1}{\partial x_2}dx_2 + \frac{\partial F_1}{\partial x_3}dx_3\right)\wedge dx_2\wedge dx_3 - \left(\frac{\partial F_2}{\partial x_1}dx_1 + \frac{\partial F_2}{\partial x_2}dx_2 + \frac{\partial F_2}{\partial x_3}dx_3\right)\wedge dx_1\wedge dx_3\right. \\
&\quad \left. + \left(\frac{\partial F_3}{\partial x_1}dx_1 + \frac{\partial F_3}{\partial x_2}dx_2 + \frac{\partial F_3}{\partial x_3}dx_3\right)\wedge dx_1\wedge dx_2\right] = \star\left[\left(\frac{\partial F_1}{\partial x_1} + \frac{\partial F_2}{\partial x_2} + \frac{\partial F_3}{\partial x_3}\right)dx_1\wedge dx_2\wedge dx_3\right] \\
&= \frac{\partial F_1}{\partial x_1} + \frac{\partial F_2}{\partial x_2} + \frac{\partial F_3}{\partial x_3} = \nabla\cdot F.
\end{aligned}$$

iv: $\star \mathrm{d}\star \mathrm{d} f = (\star \mathrm{d}\star\flat)(\sharp \mathrm{d} f) = (\star \mathrm{d}\star\flat)(\nabla f) = \nabla\cdot(\nabla f) = \Delta f.$ □

3 Whitney forms

Whenever numerical methods are used, the problem must be converted to a discrete form solvable with a computer. This includes replacing infinite-dimensional function spaces with finite-dimensional ones, whose functions can be represented in a finite basis and thus processed by computer. Since in discrete exterior calculus the problem is presented using differential forms, we are interested in finite-dimensional spaces that allow us to discretise them. The spaces we are looking for are called Whitney spaces and spanned by Whitney forms, and they are the topic of this chapter.

Lowest order Whitney forms were introduced by Whitney (1957), who called them elementary forms. These correspond to cochains on a simplicial complex. Therefore, we begin by defining a simplicial mesh, chains, and cochains in Sections 3.1 and 3.2. This enables us to present lowest order Whitney forms in Section 3.3. In Section 3.4 we introduce a new set of simplices called small simplices and use them to define higher order Whitney forms. Section 3.5 concludes how Whitney forms can be used to approximate differential forms in the finite-dimensional Whitney space. Section 3.1 follows Appendix II of Whitney (1957), and the rest of the chapter is based on the work of Rapetti and Bossavit (2009).

3.1 Simplicial mesh

A convex polyhedral cell in $\mathbb{R}^d$, or simply a cell for short, is a nonempty bounded subset that can be expressed as the intersection of finitely many closed half-spaces. The dimension of a cell is the dimension of its plane, i.e. the smallest affine subspace containing it, and cells of dimension p are called p-cells. When $p > 0$, the boundary of a p-cell σ is a union of $(p-1)$-cells. These $(p-1)$-cells are the $(p-1)$-faces of σ. Each of them may possibly have $(p-2)$-faces, each of which may have $(p-3)$-faces, and so on. All these cells are called the faces of σ. The vertices of σ are its faces of dimension 0; they are points in $\mathbb{R}^d$, and σ is the convex hull of these points.

Simplices are a special case of cells. A p-simplex s in $\mathbb{R}^d$, $0 \leq p \leq n$, is the nondegenerate convex hull of $p+1$ distinct points $n_0, \ldots, n_p \in \mathbb{R}^d$. s is a p-cell, and these points are its

vertices. Each point in s can be expressed as a sum $\lambda_0 n_0 + \ldots + \lambda_p n_p$ for some nonnegative coefficients λ_i that sum to one; the λ_i are the barycentric coordinates of the point. When $p \geq r > 0$, the convex hull of r of the vertices of s is an $(r-1)$-face of s and also an $(r-1)$-subsimplex of s.

Figure 1 has examples of simplices in the three-dimensional case. 0-simplices are just points, 1-simplices are line segments between points, 2-simplices are triangles, and 3-simplices are tetrahedra. 0-simplices are also called nodes, 1-simplices edges, 2-simplices facets, and 3-simplices volumes. This explains the labelling n_i for vertices, and labels e, f, and v are used for edges, facets, and volumes in a similar manner.

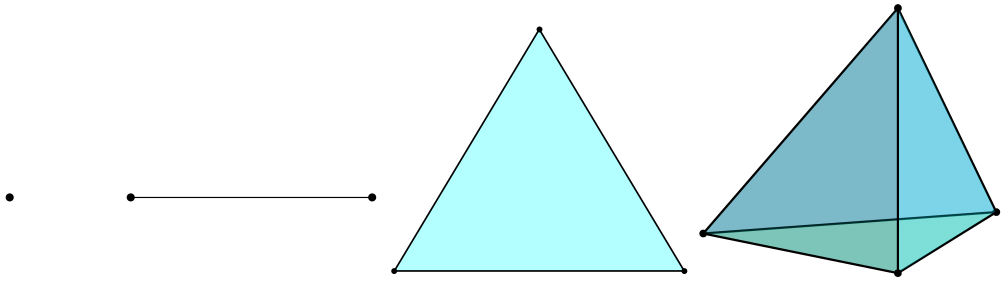

Figure 1. p-simplices with $p \in \{0,1,2,3\}$.

Suppose $p > 0$. A p-cell is oriented by orienting its plane. For p-simplices, this can be done by ordering the vertices. The notation $s = n_0 \ldots n_p$ is used for the oriented simplex whose plane is oriented by the set of vectors $(n_1 - n_0, \ldots, n_p - n_0)$. If $s' = n_{\sigma(0)} \ldots n_{\sigma(p)}$ for a permutation σ of $\{0, \ldots, p\}$, i.e. s' is the same simplex with different order of the vertices, the orientation of s' agrees with that of s if σ is even. If σ is odd, the orientations differ. Orientations that agree are considered the same, so there are two possible orientations for a p-simplex with $p > 0$. 0-simplices have two possible orientations as well, +1 and -1, and the orientation +1 is set as default.

The orientation of a p-cell induces an orientation called the induced orientation on any of its $(p-1)$-faces. When $s = n_0 \ldots n_p$ is a p-simplex with $p > 0$, the induced orientation is determined as follows. Any $(p-1)$-subsimplex s' has as vertices p of the vertices of s, i.e. s' is the convex hull of $n_0, \ldots, \widehat{n_i}, \ldots, n_p$ for some $i \in \{0, \ldots, p\}$, where the hat indicates that n_i is omitted. If i is even, $s' = n_0 \ldots \widehat{n_i}, \ldots, n_p$ with the induced orientation; if i is odd, the

opposite orientation is induced instead. If s' is equipped with the induced orientation, we say that the orientation of s' agrees with that of s.

For example, consider an edge $e = n_0n_1$. An edge is oriented by choosing a direction along it; here e is the line segment from n_0 to n_1. The induced orientation is -1 on n_0 and +1 on n_1. The orientation of a facet is a choice of a rotational direction. The edges of the facet $f = n_0n_1n_2$ with induced orientations are n_0n_1, n_1n_2, and n_2n_0. Note how each of the edges points in the same direction as the rotational direction given by the order of the vertices. Thus, it makes sense to say that their orientations agree with that of the facet.

A cell complex K is a finite set of cells such that the following conditions are fulfilled:

- Each face of any cell is also a cell in K.
- Two cells may intersect along a common face, but in no other way.

The dimension of K is the maximum of the dimensions of its cells. If all the cells in K are simplices, K is a simplicial complex. The set of points contained in at least one of the cells is called the polyhedron of K and denoted by $|K|$. We say that K is oriented if each of its cells is oriented.

Now we are ready to define a simplicial mesh. Let $D \subset \mathbb{R}^d$ be a bounded and oriented d-dimensional Riemannian manifold with piecewise smooth boundary. We define a mesh as an oriented cell complex K such that $|K|$ is a manifold. If $|K| = \bar{D}$, we say that K is a mesh in D. A simplicial mesh is a mesh whose cells are simplices. We use the notation $\mathcal{C}^p$ for the set of p-cells of the mesh.

Note that since we refer as cells to polyhedral cells, it may not be possible to find a mesh K such that $|K| = \bar{D}$. More general cell complices called CW complices could be used by attaching cells onto D through certain mappings, and a simplicial mesh in D could be defined as a triangulation of D, which exists for any smooth manifold. These are concepts of algebraic topology; see e.g. Maunder (1996) or Hatcher (2002) for more information. Instead of doing this, we relax the requirement that $|K| = \bar{D}$, assuming that $|K|$ is an approximation of D.

The adjacency relations of p-cells and $(p-1)$-cells of the mesh determine a matrix $\mathbf{D}$ of

dimension $|\mathcal{C}^p| \times |\mathcal{C}^{p-1}|$ as follows. For $\sigma_i \in \mathcal{C}^p$ and $\tau_j \in \mathcal{C}^{p-1}$, the element D_{ij} is given as:

- $D_{ij} = +1$ if τ_j is a face of σ_i and their orientations agree,
- $D_{ij} = -1$ if τ_j is a face of σ_i and their orientations differ,
- $D_{ij} = 0$ if τ_j is not a face of σ_i.

The matrix $\mathbf{D}$ is called the incidence matrix, and we denote its element linking $\sigma \in \mathcal{C}^p$ to $\tau \in \mathcal{C}^{p-1}$ by $\mathbf{D}_\tau^\sigma$. A mesh of dimension n has n incidence matrices, one for each $p \in \{1, \ldots, n\}$, linking p-cells to $(p-1)$-cells. The incidence matrix is a discrete version of the exterior derivative, as we will later see.

Whitney forms are defined on a simplicial mesh, and for this chapter it would have been sufficient to consider only simplicial meshes. But, in discrete exterior calculus meshes containing nonsimplicial cells are used as well, so to avoid repeating similar things in Chapter 4 we discussed both options here. In the rest of this chapter, we consider a d-dimensional simplicial mesh K that approximates D such that $|K| \supset D$. By simplices we refer to simplices of the mesh, and the notation $\mathcal{S}^p$ is used for the set of p-simplices.

When $n_1, \ldots, n_M$ are the nodes of the mesh, the barycentric coordinates are extended to the whole mesh as follows. Each point $p \in D$ can be expressed uniquely as a sum $p = \lambda_1 n_1 + \ldots + \lambda_M n_M$ such that whenever s is an n-simplex containing p, the λ_i corresponding to the nodes of s match the barycentric coordinates of p in s and all the other λ_i are zero. The coefficients $\lambda_1, \ldots, \lambda_M$ are the barycentric coordinates of p. When p is considered as a variable, they determine barycentric functions whose values at p are the barycentric coordinates of p. These are continuous and piecewise affine functions that sum to one at each point, and λ_i is one at the node n_i and zero at all the other nodes.

3.2 Chains and cochains

Chains are formal linear combinations of simplices. In more detail, when $0 \leq p \leq n$, a p-chain c assigns a value $c^s \in \mathbb{R}$ for each p-simplex s such that $c = \sum_{s \in \mathcal{S}^p} c^s s$. Simplices whose coefficients are negative are interpreted with the opposite orientation. If s is a p-simplex, the chain $c = s$ involving only the simplex s with coefficient one is an elementary chain

corresponding to the simplex s. We use the same symbol s to denote the simplex as well as the corresponding elementary chain.

p-cochains are the dual space to the space of p-chains, i.e. linear maps that take p-chains to $\mathbb{R}$. Since linear maps are determined by their action on the basis elements, a p-cochain b corresponds to one value $b_s \in \mathbb{R}$ per p-simplex s, and its action on the chain $c = \sum_{s \in \mathcal{S}^p} c^s s$ is given by $b(c) = \sum_{s \in \mathcal{S}^p} b_s c^s$. Both chains and cochains can be stored as vectors containing a value for each simplex. The vectors are denoted by boldface letters.

Cochains are discrete versions of differential forms. A p-form w can be integrated over p-simplices, and its integral over a p-chain is defined using linearity:

$$\int_{\sum_{s \in \mathcal{S}^p} c^s s} w = \sum_{s \in \mathcal{S}^p} c^s \int_s w.$$

This yields a cochain whose value on a p-chain is simply the integral of w over that chain. The vector corresponding to this cochain consists of integrals of w over all p-simplices. The map that takes differential forms to cochains in this way is called the de Rham map and denoted by $\mathcal{R}$.

The boundary operator ∂ takes p-chains to $(p-1)$-chains as follows. For an elementary p-chain s, ∂s is a linear combination of the $(p-1)$-faces of s. The faces whose orientations agree with that of s are given the coefficient +1, and the faces with the opposite orientation come with the coefficient -1. For a p-chain $c = \sum_{s \in \mathcal{S}^p} c^s s$ the boundary operator is then extended linearly:

$$\partial c = \partial \Big(\sum_{s \in \mathcal{S}^p} c^s s \Big) = \sum_{s \in \mathcal{S}^p} c^s \partial s.$$

Note that Stokes' theorem now extends to chains as $\int_c \mathrm{d}w = \int_{\partial c} w$. Indeed, since $\int_s \mathrm{d}w = \int_{\partial s} w$ for any p-simplex s and $(p-1)$-form w, we have that

$$\int_c \mathrm{d}w = \int_{\sum_{s \in \mathcal{S}^p} c^s s} \mathrm{d}w = \sum_{s \in \mathcal{S}^p} c^s \int_s \mathrm{d}w = \sum_{s \in \mathcal{S}^p} c^s \int_{\partial s} w = \int_{\sum_{s \in \mathcal{S}^p} c^s \partial s} w = \int_{\partial (\sum_{s \in \mathcal{S}^p} c^s s)} w = \int_{\partial c} w.$$

As the exterior derivative takes $(p-1)$-forms to p-forms and cochains are discrete differential forms, there is a discrete version of the exterior derivative, taking $(p-1)$-cochains to p-cochains. When $p > 0$ and b is a $(p-1)$-cochain, $\mathrm{d}b$ is the p-cochain acting on a p-chain

c by $\mathrm{d}b(c) = b(\partial c)$. In other words, the discrete exterior derivative is the dual of the boundary operator. Note that the condition satisfied by the discrete exterior derivative is a discrete version of Stokes' theorem: integration of forms is replaced by evaluation of cochains.

As $(p-1)$-chains and p-chains can be represented as vectors of dimension $|\mathcal{S}^{p-1}|$ and $|\mathcal{S}^p|$, the boundary operator can be represented as a matrix $\boldsymbol{\partial}$ of dimension $|\mathcal{S}^{p-1}| \times |\mathcal{S}^p|$. Similarly, the discrete exterior derivative can be represented as a matrix $\mathbf{D}$ of dimension $|\mathcal{S}^p| \times |\mathcal{S}^{p-1}|$. Note that it follows from the definitions that the matrix $\mathbf{D}$ is the incidence matrix defined in Section 3.1. Since the discrete exterior derivative is the dual of the boundary operator, their matrices are transposes of each other: $\boldsymbol{\partial} = \mathbf{D}^T$.

Example Consider the mesh in Figure 2. Its simplices are listed in Table 1.

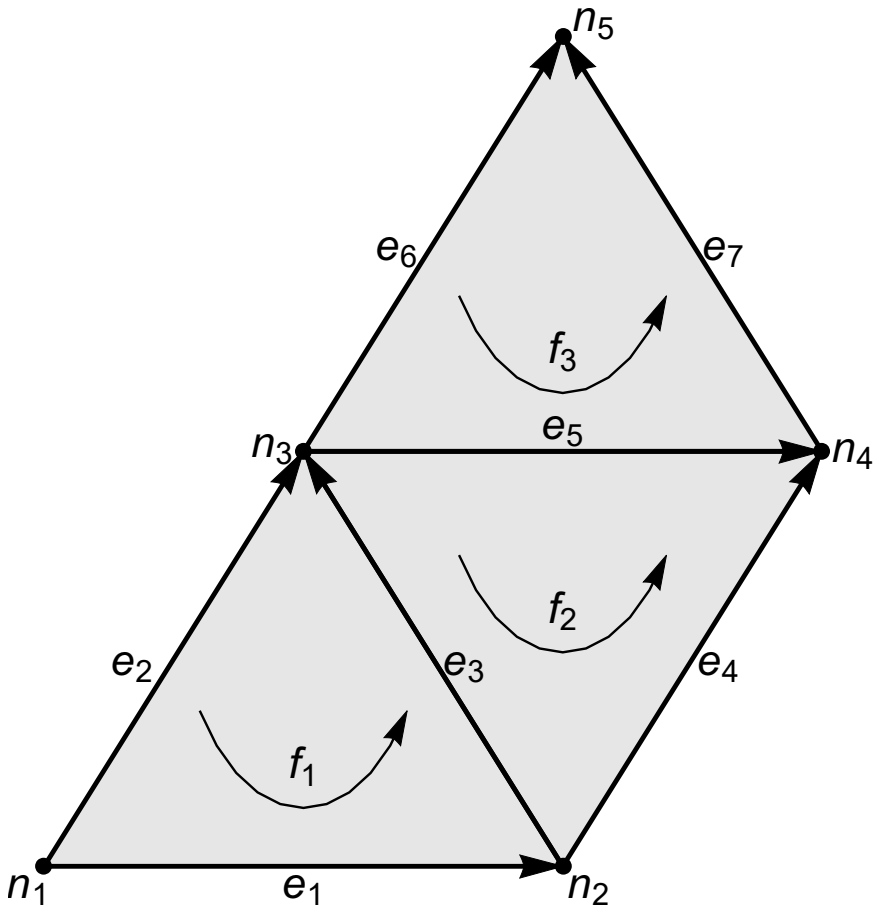

Figure 2. A two-dimensional simplicial mesh. The orientations of the simplices are illustrated with arrows.

Nodes	n_1, n_2, n_3, n_4, n_5
Edges	$e_1 = n_1n_2, e_2 = n_1n_3, e_3 = n_2n_3, e_4 = n_2n_4, e_5 = n_3n_4, e_6 = n_3n_5, e_7 = n_4n_5$
Facets	$f_1 = n_1n_2n_3, f_2 = n_2n_4n_3, f_3 = n_3n_4n_5$

Table 1. The simplices of the mesh in Figure 2.

The incidence matrices $\mathbf{D_0}$ and $\mathbf{D_1}$ linking nodes to edges and edges to facets are

$$\mathbf{D_0} = \begin{bmatrix} -1 & 1 & 0 & 0 & 0 \\ -1 & 0 & 1 & 0 & 0 \\ 0 & -1 & 1 & 0 & 0 \\ 0 & -1 & 0 & 1 & 0 \\ 0 & 0 & -1 & 1 & 0 \\ 0 & 0 & -1 & 0 & 1 \\ 0 & 0 & 0 & -1 & 1 \end{bmatrix}, \quad \mathbf{D_1} = \begin{bmatrix} 1 & -1 & 1 & 0 & 0 & 0 & 0 \\ 0 & 0 & -1 & 1 & -1 & 0 & 0 \\ 0 & 0 & 0 & 0 & 1 & -1 & 1 \end{bmatrix}.$$

The chain $c = f_1 + f_2 + f_3$ can be stored as the vector $\mathbf{c} = (1,1,1)^T$. The vector corresponding to the boundary of c is $\mathbf{D_1}^T\mathbf{c} = (1,-1,0,1,0-1,1)^T$, i.e. $\partial c = e_1 - e_2 + e_4 - e_6 + e_7$. The boundary of ∂c corresponds to the vector $\mathbf{D_0}^T\mathbf{D_1}^T\mathbf{c} = (0,0,0,0,0)^T$, so $\partial(\partial c) = 0$.

The property $\partial \circ \partial = 0$ can be shown to hold in general (see Lemma 2.1. in Hatcher 2002). Since the discrete version of the exterior derivative is the dual of the boundary operator, it follows that $\mathrm{d} \circ \mathrm{d} = 0$ holds for the discrete exterior derivative as well.

3.3 Lowest order Whitney forms

As we saw in Section 3.2, cochains are discrete versions of differential forms, given by the de Rham map $\mathcal{R}$. The Whitney map goes the other way: cochains are mapped to differential forms in the finite-dimensional space of Whitney forms. To each p-simplex s corresponds a p-form w^s, and the Whitney map, denoted by $\mathcal{P}$, maps the cochain vector $\mathbf{b}$ to the p-form $\sum_{s \in \mathcal{S}^p} b_s w^s$. An explicit formula for the p-form w^s is given in the following definition.

Definition 1 (Lowest order Whitney forms) *The differential Whitney p-form of polynomial*

degree one associated with the p-simplex $s = n_0 \dots n_p$ is

$$w^s = p! \sum_{i=0}^{p} (-1)^i \lambda_{n_i} \mathrm{d}\lambda_{n_0} \wedge \dots \wedge \widehat{\mathrm{d}\lambda_{n_i}} \wedge \dots \wedge \mathrm{d}\lambda_{n_p}, \tag{3.1}$$

where the hat indicates that $\mathrm{d}\lambda_{n_i}$ is omitted from the wedge product. For the node n, this is interpreted as $w^n = \lambda_n$. The Whitney space of p-forms is $W^p = \operatorname{span}\{w^\sigma \mid \sigma \in \mathcal{S}^p\}$.

Since in practice we will be working in a three-dimensional domain, let's see how Whitney forms look like in the case $d = 3$. The Whitney 0-form corresponding to the node n is λ_n. For the edge $e = mn$ we have that $w^e = \lambda_m \mathrm{d}\lambda_n - \lambda_n \mathrm{d}\lambda_m$. To the facet $f = lmn$ corresponds the Whitney 2-form $w^f = 2(\lambda_l \mathrm{d}\lambda_m \wedge \mathrm{d}\lambda_n - \lambda_m \mathrm{d}\lambda_l \wedge \mathrm{d}\lambda_n + \lambda_n \mathrm{d}\lambda_l \wedge \mathrm{d}\lambda_m)$. Lastly, the Whitney 3-form associated with the volume $v = klmn$ is

$$w^v = 6(\lambda_k \mathrm{d}\lambda_l \wedge \mathrm{d}\lambda_m \wedge \mathrm{d}\lambda_n - \lambda_l \mathrm{d}\lambda_k \wedge \mathrm{d}\lambda_m \wedge \mathrm{d}\lambda_n + \lambda_m \mathrm{d}\lambda_k \wedge \mathrm{d}\lambda_l \wedge \mathrm{d}\lambda_n - \lambda_n \mathrm{d}\lambda_k \wedge \mathrm{d}\lambda_l \wedge \mathrm{d}\lambda_m).$$

These Whitney forms can be identified with their proxy fields. The 0-form w^n is the piecewise affine function that is one at the node n and zero at all other nodes. To the 1-form w^e corresponds the vector field $\sharp w^e = \lambda_m \nabla\lambda_n - \lambda_n \nabla\lambda_m$, the 2-form w^f is identified with the vector field

$$\sharp \star w^f = 2(\lambda_l \nabla\lambda_m \times \nabla\lambda_n + \lambda_m \nabla\lambda_n \times \nabla\lambda_l + \lambda_n \nabla\lambda_l \times \nabla\lambda_m),$$

and with the 3-form w^v we associate the function $\star w^v = 1/|v|$. Note that for this we need a metric, since $\sharp w^e$, $\sharp \star w^f$, and $\star w^v$ are all metric dependent.

The proxy fields have appeared in the literature as finite elements with different names, often without a reference to differential forms at all. For example, the fields corresponding to edges are also known as Nédélec elements (Nédélec 1980, 1986). For more information, see Bossavit (1998, page 161) or Kirby et al. (2012, Section 3.9).

Although we required smoothness when defining differential forms in Chapter 2, here we have relaxed this requirement a little bit. We require the forms be smooth in the interior of d-simplices. In addition, p-forms should be continuous along the direction of p-simplices accross inter-element faces. Then integration on mesh elements that belong to multiple d-simplices makes sense, while the form only needs be defined almost everywhere. For more

information, see e.g. Bossavit (2005). In three dimensions 0-forms should be continuous, 1-forms tangentially continuous, and 2-forms normally continuous accross inter-element faces. Whitney forms fulfill these requirements, which is desired in application areas such as electromagnetism, elasticity, and fluid mechanics (Ainsworth and Coyle 2003).

Whitney (1957) showed that Whitney forms were defined such that the following properties hold:

- $\mathcal{P}\,\mathrm{d} = \mathrm{d}\,\mathcal{P}$,
- $\int_s w^s = 1 \;\forall s \in \mathcal{S}^p$ and $\int_{s'} w^s = 0$ for any other $s' \in \mathcal{S}^p$,
- $\mathcal{R}\mathcal{P} = \mathrm{id}$.

They are also linearly independent: if $\sum_{s\in\mathcal{S}^p} \alpha_s w^s = 0$, then $\alpha_{s'} = \int_{s'} \sum_{s\in\mathcal{S}^p} \alpha_s w^s = \int_{s'} 0 = 0$ for any $\alpha_{s'}$.

Thanks to these properties, Whitney forms are particularly handy for approximating differential forms; we return to this in Section 3.5. Although our goal is to approximate differential forms, we mention another approach to Whitney forms, which widens our understanding of them. Namely, they can be seen as tools to approximate manifolds, and approximation of differential forms is then given as a byproduct. This is discussed in the work of Bossavit (2002), which proposes a rationale for Whitney forms.

As a result, an equivalent, recursive formula for Whitney forms is given (Bossavit 2002, Proposition 1). For this we adopt the following notation: when $\sigma \in \mathcal{S}^p$ and $\tau \in \mathcal{S}^{p-1}$ is a $(p-1)$-face of σ, the node that is in σ but not in τ is denoted by $\sigma - \tau$. The corresponding barycentric function can then be denoted by $\lambda_{\sigma-\tau}$. When the 0-form w^n corresponding to the node n is defined as λ_n, the p-form associated with the p-simplex σ is given by the recursive formula

$$w^\sigma = \sum_{\tau\in\mathcal{S}^{p-1}} \mathbf{D}^\sigma_\tau \lambda_{\sigma-\tau}\,\mathrm{d}\,w^\tau, \quad 1 \le p \le d. \tag{3.2}$$

With this formula more properties of Whitney forms can be shown, as is done in the work of Rapetti and Bossavit (2009), where it's used as the definition. It's good to be aware of both possible definitions and their equivalence to avoid confusion, since both are used in the literature.

3.4 Higher order Whitney forms

Higher order Whitney forms are differential forms whose proxy fields are higher order polynomials. They can be presented in different ways (see e.g. Hiptmair 2001; Arnold, Falk, and Winther 2006; Christiansen and Rapetti 2016, and references therein). We follow the presentation of Rapetti and Bossavit (2009) based on the so-called small simplices, which are images of the mesh simplices through homothetic transformations. It turns out that with this approach we obtain higher order approximations in discrete exterior calculus with very small adaptations in the method.

For the higher order case, we consider a d-simplex σ and introduce multi-index notations. Let $\mathbf{k}$ be the array $(k_0, \ldots, k_d)$ of $d+1$ nonnegative integers, and set $k = \sum_{i=0}^{d} k_i$. Then $\mathbf{k}$ is a multi-index, and k is its weight. The set of multi-indices of weight k with $d+1$ components is denoted by $\mathcal{I}(d+1,k)$. When $\mathbf{k} \in \mathcal{I}(d+1,k)$ and $\lambda_0, \ldots, \lambda_d$ are the barycentric functions in σ, we set $\lambda^{\mathbf{k}} = \prod_{i=0}^{d} \lambda_i^{k_i}$.

For each multi-index $\mathbf{k}$ we have a map from σ onto itself, denoted by $\tilde{\mathbf{k}}$ and defined as follows. When $x \in \sigma$ and λ_i, $0 \leq i \leq d$, are its barycentric coordinates, $\tilde{\mathbf{k}}(x)$ is the point whose barycentric coordinates $\tilde{\lambda}_i$ are given as

$$\tilde{\lambda}_i = \frac{\lambda_i + k_i}{k+1}.$$

Now we can define the small p-simplices of σ: they are the images of the p-subsimplices of σ through the map $\tilde{\mathbf{k}}$. The small p-simplex $s = \tilde{\mathbf{k}}(S)$ given as the image of a p-subsimplex S through the map corresponding to the multi-index $\mathbf{k}$ is denoted by $s = \{\mathbf{k}, S\}$.

The map $\tilde{\mathbf{k}}$ is a homothety: it contracts distances by a factor of $k+1$ with respect to the point whose barycentric coordinates are $\lambda_i = k_i/k$. The small simplex $s = \{\mathbf{k}, S\}$ is similar and parallel to the subsimplex S. Note that when $d > 1$, the small d-simplices don't cover σ, and the holes left are not necessarily similar to σ. See Figures 3 and 4 for examples in two and three dimensions.

Like each p-simplex was associated with a Whitney p-form of polynomial degree one, to each small p-simplex given by a multi-index of weight k corresponds a Whitney p-form of polynomial degree $k+1$, as stated in the following definition.

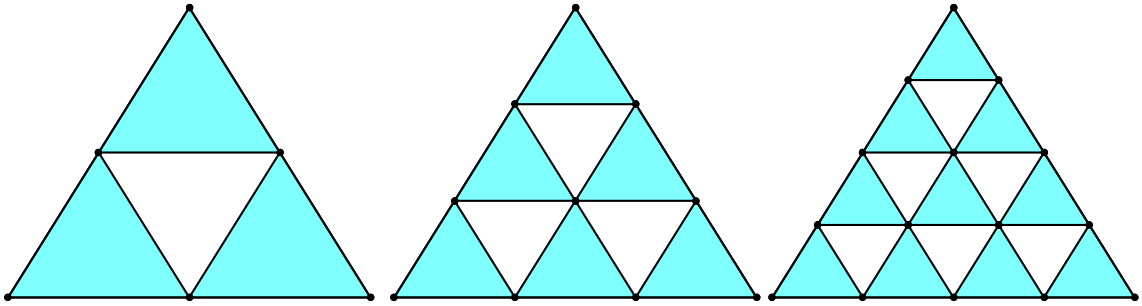

Figure 3. The small triangles $\{\mathbf{k}, f\}$ of a triangle f for all $\mathbf{k}$ in $\mathcal{I}(3,1)$, $\mathcal{I}(3,2)$, and $\mathcal{I}(3,3)$.

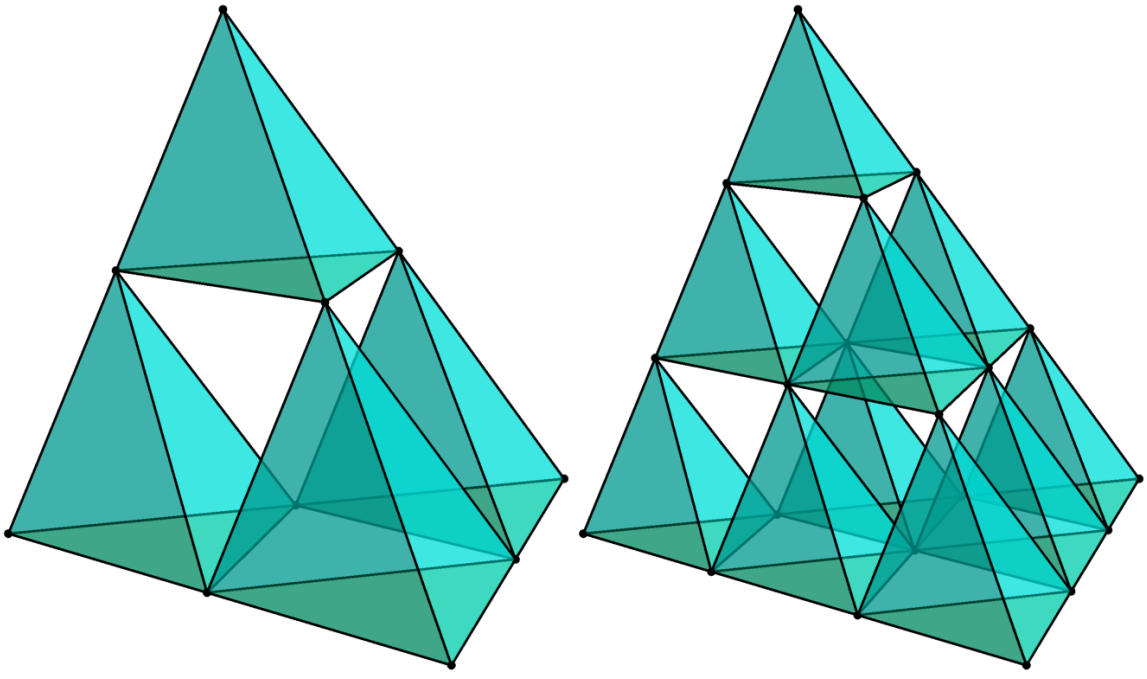

Figure 4. The small tetrahedra $\{\mathbf{k}, v\}$ of a tetrahedron v for all $\mathbf{k}$ in $\mathcal{I}(4,1)$ and $\mathcal{I}(4,2)$.

Definition 2 (Higher order Whitney forms) *Let* $\mathbf{k} = (k_0, \ldots, k_d) \in \mathcal{I}(d+1,k)$, $S \in \mathcal{S}^p$, *and let* $\{\mathbf{k}, S\}$ *be a small p-simplex of* $\sigma \in \mathcal{S}^d$. *The differential Whitney p-form of polynomial degree* $k+1$ *associated with* $\{\mathbf{k}, S\}$ *(with respect to* σ*) is*

$$w^{\{\mathbf{k},S\}} = \Big(\prod_{i=0}^{d} \lambda_i^{k_i}\Big) w^S = \lambda^{\mathbf{k}} w^S,$$

where the λ_i *are the barycentric functions with respect to* σ *and* w^S *is given by* (3.1). *The Whitney space of p-forms of polynomial degree* $k+1$, *denoted* W_{k+1}^p, *is the span of the* w^s *for all small p-simplices s of the mesh that are given by multi-indices* $\mathbf{k} \in \mathcal{I}(d+1,k)$.

When discussing the space W_{k+1}^p, by small simplices we refer to those small simplices that are given from p-simplices by multi-indices $\mathbf{k} \in \mathcal{I}(d+1,k)$ without specifying, since it's implied from context. Note that $W_1^p = W^p$: if $k = 0$, the components of $\mathbf{k}$ are all zero and $w^{\{\mathbf{k},S\}} = w^S$. Since the forms spanning W_{k+1}^p are products between an element in W^p and the continuous function $\lambda^{\mathbf{k}}$, the elements in W_{k+1}^p possess the same conformity properties as those in W^p.

Example Consider the three-dimensional case $d = 3$ and the tetrahedron $v = klmn$. Then $w^{\{(0,1,0,0),k\}} = \lambda_l w^k = \lambda_l \lambda_k$ is a second order Whitney 0-form,

$$w^{\{(1,0,0,1),lmn\}} = \lambda_k \lambda_n w^{lmn} = 2\lambda_k \lambda_n (\lambda_l \,\mathrm{d}\lambda_m \wedge \mathrm{d}\lambda_n - \lambda_m \,\mathrm{d}\lambda_l \wedge \mathrm{d}\lambda_n + \lambda_n \,\mathrm{d}\lambda_l \wedge \mathrm{d}\lambda_m)$$

is a third order Whitney 2-form, and $w^{\{(1,0,2,0),kl\}} = \lambda_k \lambda_m^2 w^{kl} = \lambda_k \lambda_m^2 (\lambda_k \,\mathrm{d}\lambda_l - \lambda_l \,\mathrm{d}\lambda_k)$ is a fourth order Whitney 1-form.

Although they span W_{k+1}^p, the p-forms of order $k+1$ given in Definition 2 don't constitute a basis since they are not linearly independent. This follows from the following proposition.

Proposition 1 *Let* $1 \le p \le d$. *For any p-simplex* $\sigma \in \mathcal{S}^p$ *we have that*

$$\sum_{\tau \in \mathcal{S}^{p-1}} \mathbf{D}_\tau^\sigma \lambda_{\sigma-\tau} w^\tau = 0. \tag{3.3}$$

Proof. The case $p = 1$ is obvious: for the edge kl we have

$$\sum_{n \in \mathcal{S}^0} \mathbf{D}_n^e \lambda_{e-n} w^n = \lambda_k \lambda_l - \lambda_l \lambda_k = 0.$$

For $p > 1$, using the recursive formula (3.2) we get

$$\sum_{\tau\in\mathcal{S}^{p-1}} \mathbf{D}^\sigma_\tau \lambda_{\sigma-\tau} w^\tau = \sum_{\tau\in\mathcal{S}^{p-1}} \mathbf{D}^\sigma_\tau \lambda_{\sigma-\tau} \sum_{\upsilon\in\mathcal{S}^{p-2}} \mathbf{D}^\tau_\upsilon \lambda_{\tau-\upsilon}\,\mathrm{d}\,w^\upsilon = \sum_{\upsilon\in\mathcal{S}^{p-2}} \sum_{\tau\in\mathcal{S}^{p-1}} \lambda_{\sigma-\tau}\lambda_{\tau-\upsilon}\mathbf{D}^\sigma_\tau \mathbf{D}^\tau_\upsilon\,\mathrm{d}\,w^\upsilon.$$

Fix $\upsilon \in \mathcal{S}^{p-2}$. $\mathbf{D}^\sigma_\tau \mathbf{D}^\tau_\upsilon \neq 0$ only if $\upsilon \subset \tau \subset \sigma$, which is possible only if υ is a subsimplex of σ. In this case, let m and n be the two nodes of σ that are not in υ. Then $\sigma - \tau$ must be one of them and $\tau - \upsilon$ the other, so $\lambda_{\sigma-\tau}\lambda_{\tau-\upsilon} = \lambda_m\lambda_n$. Since $\mathbf{D_{p-1}D_{p-2}} = 0$, we have

$$\sum_{\tau\in\mathcal{S}^{p-1}} \lambda_{\sigma-\tau}\lambda_{\tau-\upsilon}\mathbf{D}^\sigma_\tau \mathbf{D}^\tau_\upsilon = \sum_{\tau\in\mathcal{S}^{p-1}} \lambda_m\lambda_n \mathbf{D}^\sigma_\tau \mathbf{D}^\tau_\upsilon = 0,$$

and the claim follows. □

The linear dependency of second order forms follows immediately from (3.3), and for forms of order $k > 2$ it is seen by multiplying the equation by $\lambda^{\mathbf{k}}$ for any $\mathbf{k} \in \mathcal{I}(d+1, k-2)$. For example, multiplying the equation by λ_n gives

$$\sum_{\tau\in\mathcal{S}^{p-1}} \mathbf{D}^\sigma_\tau \lambda_n \lambda_{\sigma-\tau} w^\tau = 0$$

when n is any node of σ, and this shows the linear dependency of third order forms.

Which forms are linearly dependent can be seen from (3.3), and some of those can be discarded to obtain a basis for W^p_{k+1}. This will be illustrated with examples in Chapter 5 when we consider the implementation of second order approximations.

3.5 Whitney forms as approximations for differential forms

Now we have the tools to approximate differential forms: a simplicial mesh, the Whitney spaces it induces, and the maps $\mathcal{R}$ and $\mathcal{P}$. In this chapter we conclude how approximating is done, starting with the lowest order case, and observe how things have to be adapted when higher order forms are used.

Suppose that we wish to approximate a p-form ω in the Whitney space W^p. Since lowest order Whitney p-forms constitute a basis for W^p, any element w in this space can be written uniquely as a sum $w = \sum_{s\in\mathcal{S}^p} \alpha_s w^s$ for some coefficients α_s. The coefficients are called degrees of freedom, and w can be identified with the cochain $b = \mathcal{R}w$ or the corresponding cochain vector $\mathbf{b}$ whose components are the α_s.

As mentioned in the introduction, we can integrate ω over all p-simplices of the mesh and consider the vector of the integrals as a discrete version of ω. The vector given this way is exactly the cochain vector corresponding to the cochain $\mathcal{R}\omega$. It can be identified with the Whitney form $\mathcal{PR}\omega = \sum_{s\in\mathcal{S}^p}(\int_s \omega)w^s = \sum_{s\in\mathcal{S}^p}\alpha_s w^s$, where $\alpha_s = \int_s \omega$. Thus, the approximation is $\mathcal{PR}\omega$, and the degrees of freedom are the integrals over all p-simplices of the mesh.

Recall that $\mathcal{RP} = \mathrm{id}$, so if we start with an element in the finite-dimensional space of cochains, we don't lose information when it's mapped to W^p and back. Similarly, if $w = \sum_{s\in\mathcal{S}^p}\alpha_s w^s \in W^p$, then

$$\mathcal{PR}w = \sum_{s'\in\mathcal{S}^p}\left(\int_{s'}\sum_{s\in\mathcal{S}^p}\alpha_s w^s\right)w^{s'} = \sum_{s'\in\mathcal{S}^p}\alpha_{s'}w^{s'} = w,$$

so the approximation is exact, but in general $\mathcal{PR}$ is not the identity. This is the price we have to pay when the infinite-dimensional space $\Omega^p(D)$ is replaced with W^p. However, when the mesh grain tends to zero, the accuracy of the approximations increases, and it can be shown that $\mathcal{PR}\to\mathrm{id}$ when the mesh is refined in a suitable way (Bossavit 1998; Dodziuk 1976).

Another property mentioned earlier is $\mathcal{P}\,\mathrm{d} = \mathrm{d}\,\mathcal{P}$, which can also be written as $\mathcal{P}\mathbf{D} = \mathrm{d}\,\mathcal{P}$ when cochains are identified with cochain vectors. This implies that

$$\mathrm{d}\,w^\tau = \sum_{\sigma\in\mathcal{S}^{p+1}}\mathbf{D}^\sigma_\tau w^\sigma \quad \forall\tau\in\mathcal{S}^p,$$

so in particular $\mathrm{d}\,W^p \subset W^{p+1}$. Moreover, $\mathcal{R}\,\mathrm{d} = \mathrm{d}\,\mathcal{R}$, i.e. $\mathcal{R}\,\mathrm{d} = \mathbf{D}\mathcal{R}$, which follows immediately from $\boldsymbol{\partial} = \mathbf{D}^T$ and Stokes' theorem. Therefore, the exterior derivative is exact in that we can first approximate ω and then apply the incidence matrix to the cochain vector or approximate $\mathrm{d}\,\omega$ with the same result.

So, approximating and discretising differential forms with lowest order Whitney forms and the corresponding cochains is simple, but with higher order forms things get more complicated. First of all, any element in W^p_k can be written as a sum $\sum_s \alpha_s w^s$, where the sum is over all small simplices of the mesh, but this expression is not unique, since the kth order p-forms are not linearly independent. Secondly, it is not true that $\int_s w^s = 1$ and $\int_s w^{s'} = 0$ for all small simplices $s' \neq s$, so we don't have $\mathcal{RP} = \mathrm{id}$ for cochains over small simplices.

To deal with this, first consider a mesh with a single d-simplex σ. We can integrate the forms spanning W_k^p over all small simplices and form a matrix A, indexed over small simplices, such that $A^s_{s'}$, the element in the s-row and the s'-column, is the integral $\int_s w^{s'}$. Note that for cochains over small simplices we have $A = \mathcal{R}\mathcal{P}$. The matrix A is singular since the forms are linearly dependent, but if we pick some of them to obtain a basis for W_k^p and only consider the small simplices corresponding to these, A becomes invertible. This is because of the unisolvence property stated by Rapetti and Bossavit (2007, 2009).

Then, for cochains over these small simplices, we have $\mathcal{R}\mathcal{P}A^{-1} = A^{-1}\mathcal{R}\mathcal{P} = \mathrm{id}$, and for $w = \sum_s \alpha_s w^s \in W_k^p$ we have $\mathcal{P}A^{-1}\mathcal{R}w = w$, since the s-component of the cochain vector $A^{-1}\mathcal{R}w$ is α_s:

$$(A^{-1}\mathcal{R}w)_s = \sum_{s'}(A^{-1})^s_{s'}\int_{s'} w = \sum_{s'}(A^{-1})^s_{s'}\int_{s'}\sum_{s''}\alpha_{s''}w^{s''} = \sum_{s''}\alpha_{s''}\sum_{s'}(A^{-1})^s_{s'}A^{s'}_{s''} = \sum_{s''}\alpha_{s''}\delta^s_{s''} = \alpha_s.$$

Therefore, we can approximate a p-form ω with $\mathcal{P}A^{-1}\mathcal{R}\omega$, and for elements in W_k^p the approximation is exact. The degrees of freedom are now integrals over linear combinations of small simplices: $\mathcal{P}A^{-1}\mathcal{R}\omega = \sum_s \alpha_s w^s$, where $\alpha_s = \sum_{s'}(A^{-1})^s_{s'}\int_{s'}\omega$.

It turns out that the same strategy can be used for meshes with multiple d-simplices. Any small simplex is contained in some d-simplex σ, and to preserve the properties stated above we wish to define the coefficient α_s as $\alpha_s = \sum_{s'}(A^{-1})^s_{s'}\int_{s'}\omega$, where the sum is over small simplices of σ. A potential issue here is that when $p < d$, some small p-simplices are contained in multiple d-simplices, and α_s could depend on the choice of σ. It is not obvious that α_s is well-defined.

To see that this indeed is the case, we must show that if s is a small simplex contained in two d-simplices σ and σ', then $(A^{-1})^s_{s'} = 0$ for those small simplices s' of σ that are not contained in σ' as well. Then it's easy to see that $\alpha_s = \sum_{s'}(A^{-1})^s_{s'}\int_{s'}\omega$ is the same, whether the sum is taken over small simplices of σ or σ'.

So suppose that s and s' are small simplices of the d-simplex σ and σ' is another d-simplex containing s but not s'. Then σ and σ' intersect along a common face $\tau = \sigma \cap \sigma'$ that contains s but not s'. If $s' = \{\mathbf{k}, S\}$ and S is a subsimplex of σ contained in τ, then $w^{s'}$ has as a factor at least one of the barycentric functions corresponding to nodes that are in σ but not in τ.

Since these are all zero in τ, so is $w^{s'}$, and thus $\int_s w^{s'} = 0$. If S is not in τ, then $w^{s'} = 0$ in the interior of σ', and $\int_s w^{s'} = 0$ follows from the inter-element continuity along the direction of s.

Let $\{s, s_1, \ldots, s_N\}$ be the set of small simplices of σ that are also in σ', and let P be a permutation matrix such that these are indexed last in the matrix PAP. Since $A^{s''}_{s'} = \int_{s''} w^{s'} = 0$ whenever $s'' \in \{s, s_1, \ldots, s_N\}$ and s' is a small simplex of σ not in σ', the matrix PAP is block upper triangular. Its inverse $(PAP)^{-1} = PA^{-1}P$ has the same upper triangular block structure, so we see that $(A^{-1})^s_{s'} = 0$, as desired.

The above described construction for higher order approximations may seem technical at first glance, but we stress its naturality by comparing to the lowest order case: with lowest order Whitney forms, the integrals of the approximation match with those of the initial function over the mesh simplices. In the higher order case, we cannot find an element that has the same integrals as the initial function over all of the small simplices, but after we omit some of them to deal with the linear dependency of the forms, we obtain an approximation whose integrals coincide with those of the initial function over the rest of the small simplices.

One more thing to consider is how the exterior derivative behaves with these approximations. The boundary of small $(p+1)$-simplices consists of small p-simplices, so we have the boundary operator ∂, the discrete exterior derivative d, and the respective matrices $\boldsymbol{\partial}$ and $\mathbf{D}$ for chains and cochains over small simplices. But, while previously only some of the small simplices were considered to obtain linear independency, we now have to include them all for ∂ and d to make sense.

Then $\mathcal{R}\,\mathrm{d} = \mathbf{D}\mathcal{R}$ follows again from $\boldsymbol{\partial} = \mathbf{D}^T$ and Stokes' theorem, and for a p-form ω we have $\mathcal{P}A^{-1}\mathcal{R}\,\mathrm{d}\,\omega = \mathcal{P}A^{-1}\mathbf{D}\mathcal{R}\omega$ if we drop the redundant small simplices before applying the matrix A^{-1}. This will be our strategy in discrete exterior calculus: to preserve the necessary structures we keep track of all small simplices, but when we wish to write the solution in the chosen basis, the redundant small simplices are discarded.

4 Discrete exterior calculus

As mentioned in the introduction, discrete exterior calculus is the numerical partial differential equation solving method that we consider in this thesis. It can be seen as a generalisation of Yee's FDTD method (1966) in computational electromagnetism (Bossavit and Kettunen 1999). Its applications include wave propagation problems not only in electromagnetism, but also related to sound propagation, elastic waves, and quantum mechanics (Räbinä et al. 2018).

Discrete exterior calculus is a wide topic, and for this thesis we have to harshly limit the scope of discussion. The goal of this chapter is to give an idea how discrete exterior calculus works with the help of an example. For this we consider a numerical solution of Maxwell's equations in the three-dimensional Euclidean space, following the work of Räbinä (2014), which can be consulted for more details. For a more general and theoretical viewpoint of discrete exterior calculus, see Desbrun et al. (2005), Grady and Polimeni (2010), and the references therein.

The model problem we consider is given by Maxwell's equations

$$\begin{aligned}
\nabla \times \vec{E} &= -\frac{\partial \vec{B}}{\partial t}, \\
\nabla \times \vec{H} &= \frac{\partial \vec{D}}{\partial t} + \vec{J}, \\
\vec{D} &= \varepsilon \vec{E}, \\
\vec{B} &= \mu \vec{H}, \\
\vec{J} &= \sigma \vec{E}.
\end{aligned}$$

The vector fields $\vec{E}$, $\vec{H}$, $\vec{D}$, and $\vec{B}$ represent electric and magnetic fields and electric and magnetic flux densities, and the scalar fields ε and μ represent permittivity and permeability of the medium. $\vec{J}$ is a vector field representing electric current density, and the scalar field σ represents electric conductivity of the medium.

In discrete exterior calculus, partial differential equations are formulated in terms of differential forms. Recall that the example of Section 2.4 showed how this can be done. In this

case we replace the vector fields $\vec{E}$ and $\vec{H}$ with the 1-forms $e = \flat\vec{E}$ and $h = \flat\vec{H}$, and $\vec{D}$, $\vec{B}$, and $\vec{J}$ with the 2-forms $d = \star\flat\vec{D}$, $b = \star\flat\vec{B}$, and $j = \star\flat\vec{J}$. The problem then reads

$$\mathrm{d}e = -\partial_t b, \tag{4.1}$$

$$\mathrm{d}h = \partial_t d + j, \tag{4.2}$$

$$d = \varepsilon \star e, \tag{4.3}$$

$$b = \mu \star h, \tag{4.4}$$

$$j = \sigma \star e. \tag{4.5}$$

Equation (4.1) is known as Faraday's law and (4.2) as Ampere's law. The relations (4.3), (4.4), and (4.5) are called the constitutive relations.

4.1 Spatial discretisation

Next, the problem represented with differential forms is discretised. The spatial discretisation is done using two 3-dimensional meshes, primal and dual mesh. The definition of mesh here is the same as in Section 3.1, so it consists of convex polyhedral cells. For now, the mesh doesn't necessarily have to be simplicial, but since a simplicial primal mesh is assumed later so that Whitney forms are defined, it is used in examples here as well.

To each p-cell c corresponds a dual cell $*c$, which is a $(3-p)$-cell. The dual mesh is a mesh consisting of the dual cells of the cells in the primal mesh K. The dual cells fulfill the following condition: if c^{p-1} is a $(p-1)$-face of c^p, then $*c^p$ is a $(3-p)$-face of $*c^{p-1}$. We point out that if c is on the boundary of $|K|$, the dual cell of c is not a cell by definition because its boundary is not complete. In this case we take its intersection with $|K|$ to complete the boundary.

Each node, edge, facet, and volume in the dual mesh is a dual cell of a volume, facet, edge, and node (respectively) in the primal mesh. The orientations for dual cells can be chosen such that the incidence matrices $*\mathbf{D}$ of the dual mesh are the transposes of those of the primal mesh: $*\mathbf{D_0} = \mathbf{D_2}^T$, $*\mathbf{D_1} = \mathbf{D_1}^T$, and $*\mathbf{D_2} = \mathbf{D_0}^T$.

In Figure 5 we have an example of how primal and dual mesh elements may look like. The primal volume is a tetrahedron. In the left we have highlighted one primal node and its dual

cell, which is a truncated octahedron. In the middle, two primal edges and their dual facets are highlighted, and in the right we have highlighted a primal facet and its dual edge.

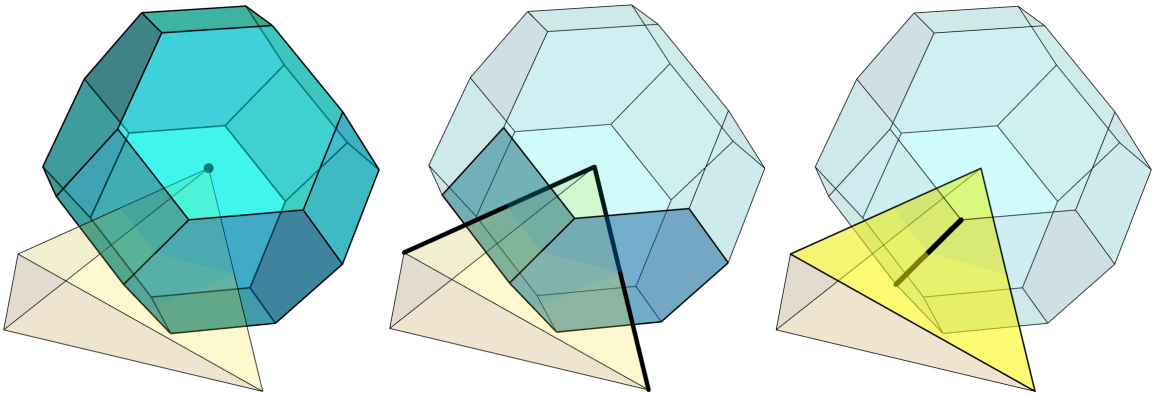

Figure 5. Examples of primal and dual cells.

The dual mesh is needed for discretising the Hodge star operator. The forms e and b are discretised on the primal mesh and the forms h, d, and j on the dual mesh. Operating with the Hodge star can then be seen as moving from one mesh to another. This will be explained in Section 4.2.

The forms are discretised as follows. e is integrated over primal edges, which yields an array $\mathbf{e}$ indexed over the edges. Each component of the array is the integral of e over the corresponding edge. Similarly, we integrate b over primal facets, h over dual edges, and d and j over dual facets to yield arrays $\mathbf{b}$, $\mathbf{h}$, $\mathbf{d}$, and $\mathbf{j}$.

Note that if the meshes were simplicial, the arrays would be the cochain vectors corresponding to lowest order Whitney forms. The discretisation would be done as we explained in Section 3.5. In the general case the arrays don't correspond to Whitney forms, but even then they can be seen as cochain vectors if we define the chains and cochains on the space of more general cells. For this reason, we call the arrays cochain vectors and use the same boldface notation as before.

4.2 Discrete Hodge star

We have already seen that the incidence matrix is the discrete version of the exterior derivative. In this section, we introduce a discrete version of the Hodge star operator. Like the incidence matrix, it will be a matrix that operates on cochain vectors.

Recall that the Hodge star maps p-forms to $(3-p)$-forms. The discrete Hodge star should therefore map p-cochain vectors to $(3-p)$-cochain vectors. In other words, when we know the integrals of ω over p-cells, the discrete Hodge should give us the integrals of $\star\omega$ over $(3-p)$-cells.

This is achieved with the help of the dual mesh. If ω is discretised on the primal mesh, $\star\omega$ is discretised on the dual mesh. The dual cell of a p-cell is a $(3-p)$-cell, so when we know the integrals of ω over p-cells, the discrete Hodge star should give us the integrals of $\star\omega$ over their dual cells. They can be determined approximately as follows.

Let's consider the relation $d = \varepsilon \star e$, which originated from $\vec{D} = \varepsilon\vec{E}$. The integral of e over the primal edge c is

$$\int_c e = \int_c \vec{E} \cdot t_c,$$

where by t_c we denote the unit tangent vector of c. The integral of $\star e$ over the dual facet $*c$ on the other hand is

$$\int_{*c} \star e = \int_{*c} \vec{E} \cdot n_{*c},$$

where n_{*c} is now the unit normal vector of $*c$. If we assume $t_c = n_{*c}$ and approximate the field locally as constant, we have

$$\int_{*c} \star e = \int_{*c} \vec{E} \cdot n_{*c} = |*c|\vec{E} \cdot n_{*c} = |*c|\vec{E} \cdot t_c = \frac{|*c|}{|c|}\int_c \vec{E} \cdot t_c = \frac{|*c|}{|c|}\int_c e,$$

which leads to a diagonal discrete Hodge matrix with diagonal elements $\star_{ii} = \frac{|*c_i|}{|c_i|}$.

When $0 \leq p \leq 3$, we denote by $\star_p$ the discrete Hodge star matrix mapping p-cochain vectors on the primal mesh to $(3-p)$-cochain vectors on the dual mesh. The matrices $\star_0$, $\star_2$, and $\star_3$ are determined similarly as $\star_1$ above. Note that in three dimensions $\star\star\,\omega = \omega$ for a p-form ω with any $p \in \{0,1,2,3\}$, so the Hodge operator mapping $(3-p)$-forms to p-forms is the

inverse of the Hodge operator mapping p-forms to $(3-p)$-forms. Therefore, the inverse of the matrix $\star_p$ is the right discrete Hodge operator for a $(3-p)$-form that is discretised on the dual mesh.

Diagonal Hodge matrices are particularly convenient since their inverses are trivial to compute and the matrix-vector multiplication is computationally cheap as well. However, this approximation requires two properties from the dual cells: orthogonality and good relative alignment. Orthogonality means that each vector of the dual cell $*c$ is orthogonal to each vector of c. This is needed because we assumed $t_c = n_{*c}$. In addition, the centres of the cells should be close to each other so that approximating the forms locally as constants makes sense. These requirements are illustrated in Figure 6. How to build the two meshes such that these properties are satisfied is not discussed here, but we emphasise that mesh generation is an important part of discrete exterior calculus and significantly affects the efficiency of the solution method.

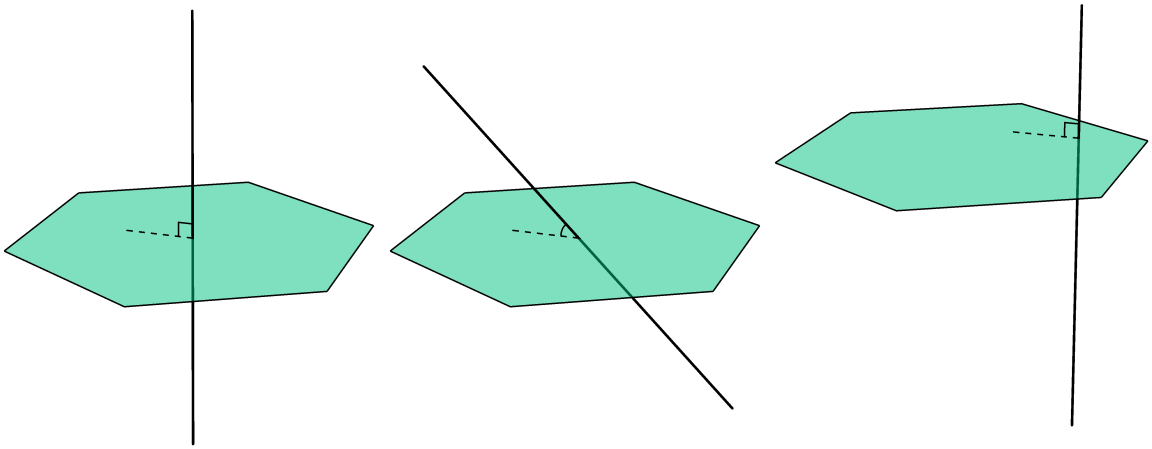

Figure 6. The primal and dual cell in the left fulfill the requirements of orthogonality and good relative alignment. In the middle they are not orthogonal, while in the right their centres are poorly positioned relative to each other.

By assuming ε and μ locally constant as well, the discrete versions of the constitutive relations (4.3) and (4.4) can be written as $\mathbf{d} = \varepsilon \star_1 \mathbf{e}$ and $\mathbf{b} = \mu \star_2^{-1} \mathbf{h}$, where ε and μ are now diagonal matrices whose elements ε_{ii} and μ_{jj} represent the values of ε and μ around the corresponding cells i and j. These can be coupled with the Hodge matrices by writing

$\star_\varepsilon = \varepsilon\star_1$ and $\star_\mu = \mu^{-1}\star_2$. Similarly, by approximating σ locally as constant, the equation (4.5) is written as $\mathbf{j} = \sigma\star_1\mathbf{e} = \star_\sigma\mathbf{e}$, where σ is a diagonal matrix and $\star_\sigma = \sigma\star_1$. The discrete version of the problem can now be written as

$$\begin{aligned}
&\mathbf{D_1}\mathbf{e} = -\partial_t\mathbf{b},\\
&\mathbf{D_1}^T\mathbf{h} = \partial_t\mathbf{d} + \mathbf{j},\\
&\mathbf{d} = \star_\varepsilon\mathbf{e},\\
&\mathbf{b} = \star_\mu^{-1}\mathbf{h},\\
&\mathbf{j} = \star_\sigma\mathbf{e},
\end{aligned}$$

where $\mathbf{D_1}$ is the incidence matrix linking primal edges to primal facets. We can also eliminate $\mathbf{d}$, $\mathbf{h}$, and $\mathbf{j}$ from the equations: since $\mathbf{d} = \star_\varepsilon\mathbf{e}$, $\mathbf{h} = \star_\mu\mathbf{b}$, and $\mathbf{j} = \star_\sigma\mathbf{e}$, the problem can be written with just $\mathbf{e}$ and $\mathbf{b}$ as

$$\begin{aligned}
&\mathbf{D_1}\mathbf{e} = -\partial_t\mathbf{b},\\
&\mathbf{D_1}^T\star_\mu\mathbf{b} = \partial_t\star_\varepsilon\mathbf{e} + \star_\sigma\mathbf{e}.
\end{aligned} \tag{4.6}$$

4.3 Time integration

Time integration is a term used for solving the equations by tracking wave propagation forward in time. This is done by approximating the time derivatives with finite difference approximations. Let Δt denote the time step length, t_0 the initial time, and t_k the time instance $t_0 + k\Delta t$. We evaluate the values of $\mathbf{e}$ at time instances $t_k + \frac{\Delta t}{2}$ and the values of $\mathbf{b}$ at time instances t_k. Then the equations (4.6) can be discretised in time as

$$\begin{aligned}
\mathbf{D_1}\mathbf{e}\left(t_k + \frac{\Delta t}{2}\right) &= -\frac{\mathbf{b}(t_{k+1}) - \mathbf{b}(t_k)}{\Delta t},\\
\mathbf{D_1}^T\star_\mu\mathbf{b}(t_k) &= \frac{\star_\varepsilon\mathbf{e}\left(t_k + \frac{\Delta t}{2}\right) - \star_\varepsilon\mathbf{e}\left(t_k - \frac{\Delta t}{2}\right)}{\Delta t} + \star_\sigma\mathbf{e}(t_k).
\end{aligned}$$

Since $\mathbf{e}$ is defined at time instances $t_k + \frac{\Delta t}{2}$, we approximate its value at t_k with

$$\mathbf{e}(t_k) = \frac{\mathbf{e}\left(t_k - \frac{\Delta t}{2}\right) + \mathbf{e}\left(t_k + \frac{\Delta t}{2}\right)}{2}.$$

When this is substituted into the second equation, we get the value update equations for $\mathbf{e}$ and $\mathbf{b}$:

$$\mathbf{b}(t_{k+1}) = \mathbf{b}(t_k) - \Delta t \mathbf{D_1} \mathbf{e}\left(t_k + \frac{\Delta t}{2}\right), \tag{4.7}$$

$$\mathbf{e}\left(t_k + \frac{\Delta t}{2}\right) = \mathbf{e}\left(t_k - \frac{\Delta t}{2}\right) + \left(\frac{\star_\varepsilon}{\Delta t} + \frac{\star_\sigma}{2}\right)^{-1} \left(\mathbf{D_1}^T \star_\mu \mathbf{b}(t_k) - \star_\sigma \mathbf{e}\left(t_k - \frac{\Delta t}{2}\right)\right). \tag{4.8}$$

The initial values $\mathbf{e}(t_0 - \frac{\Delta t}{2})$ and $\mathbf{b}(t_0)$ are assumed to be known, so we can use (4.8) to determine $\mathbf{e}(t_0 + \frac{\Delta t}{2})$. With this we can update the value of $\mathbf{b}$ using (4.7), and the new value of $\mathbf{b}$ can then be used to update $\mathbf{e}$ with (4.8). This process is then repeated: the values of $\mathbf{b}$ and $\mathbf{e}$ are updated in turn using the value update equations (4.7) and (4.8), and wave propagation can be tracked forward in time. This method to solve the equations in time is called the leapfrog time stepping scheme.

The time step length Δt has to be short enough for the stability of the time stepping scheme. If it's too long, the values of $\mathbf{e}$ and $\mathbf{b}$ start bouncing between positive and negative values and the absolute values grow without bound. The limit for the time step length is known as the CFL condition. To obtain stability for the time stepping scheme, the step length must be chosen such that

$$\Delta t < \frac{2}{\sqrt{\chi}},$$

where χ is the largest eigenvalue of the matrix $\star_\varepsilon^{-1} \mathbf{D_1}^T \star_\mu \mathbf{D_1}$.

The CFL limit depends on the speed of the wave and the mesh grain. When the mesh grain decreases or the wave speed increases, the maximum time step length allowed becomes shorter. The time step length must satisfy the CFL condition but should not be chosen too short, or the iteration process becomes inefficient due to unnecessary consumption of time.

The solution obtained at each time instance is a cochain vector; we know the integrals of $\mathbf{e}$ over primal edges and the integrals of $\mathbf{b}$ over primal facets. The forms e and b have to be constructed from these with some kind of interpolation. When we restrict to simplicial meshes, the solution corresponds to a lowest order Whitney form and the interpolation is done with the Whitney map, as already discussed. To interpolate with higher order Whitney

forms we would need the integrals over small simplices. The idea is to form a simplicial mesh, divide it into small simplices, and solve the problem on the refined mesh. This will be covered in more detail in Section 5.4, where we show how second order Whitney forms are used in discrete exterior calculus.

5 Second order approximations

Now we have sufficiently covered the theory of Whitney forms and discrete exterior calculus, and it's time for the practical part of the thesis. In this chapter we consider the implementation of second order Whitney forms on a DEC-based wave simulation software. We first use them to approximate differential forms in one-, two-, and three-dimensional spaces. This illustrates the discussion of Section 3.5, since we see how the approximations are done in practice. Then, in Section 5.4, we show how to use second order Whitney forms in discrete exterior calculus and solve the model problem of Chapter 4.

In the second order case we can simplify our notation as follows. Since multi-indices have now weight 1, one of their component is 1 and the others are 0. Therefore, we can identify them with the corresponding nodes. For example, the small edge $s = \{(0,1,0,0), lk\}$ of the volume $mnlk$ can be expressed more succinctly as $s = \{n, lk\}$.

5.1 One-dimensional case

In one dimension, the mesh has only edges and nodes. The edge $e = mn$ has 4 small nodes and 2 small edges (see Figure 7). The forms $w^{\{m,n\}} = \lambda_m \lambda_n$ and $w^{\{n,m\}} = \lambda_n \lambda_m$ are linearly dependent; in fact, the forms and the corresponding small nodes are exactly the same. We can simply drop the small node $\{n,m\}$ so that the two small nodes at the midedge are considered the same.

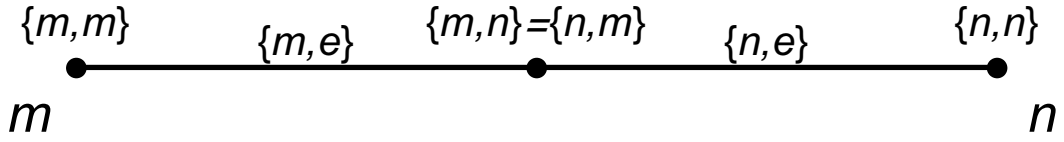

Figure 7. The small simplices of the edge $e = mn$. There are two small nodes at the midedge, but these will be considered the same.

The small simplices and the corresponding forms are given the indexing shown in Table 2. The indexing is interpreted such that s_i is the small simplex whose index is i and w^j is the

the form corresponding to the small simplex whose index is j. An orientation for the small edges is implied: for example, $\{m,e\}$ points in the same direction as e.

Small nodes	
$\{m,m\} \leftarrow 1$	~~$\{n,m\}$~~
$\{m,n\} \leftarrow 2$	$\{n,n\} \leftarrow 3$

Small edges	
$\{m,e\} \leftarrow 1$	$\{n,e\} \leftarrow 2$

Table 2. Indexing of the small simplices of the edge $e = mn$.

Next, we compute the matrices A whose elements A_{ij} are given as $A_{ij} = \int_{s_i} w^j$. Let's denote by A_n the matrix A for small nodes and by A_e for small edges. Note that in one dimension the proxy field of the lowest order Whitney 1-form corresponding to the edge $e = mn$ is $\sharp w^e = \lambda_m \nabla \lambda_n - \lambda_n \nabla \lambda_m$, which is $\frac{1}{|e|}$ in e and zero outside e. With this in mind, the matrices are easy to compute and they read

$$A_n = \frac{1}{4} \begin{bmatrix} 4 & 0 & 0 \\ 1 & 1 & 1 \\ 0 & 0 & 4 \end{bmatrix}, \quad A_e = \frac{1}{8} \begin{bmatrix} 3 & 1 \\ 1 & 3 \end{bmatrix}.$$

Their inverses are

$$A_n^{-1} = \begin{bmatrix} 1 & 0 & 0 \\ -1 & 4 & -1 \\ 0 & 0 & 1 \end{bmatrix}, \quad A_e^{-1} = \begin{bmatrix} 3 & -1 \\ -1 & 3 \end{bmatrix}.$$

As discussed in Section 3.5, a p-form can be approximated as $\sum_s \alpha_s w^s$, where the sum is over small p-simplices. Now $p \in \{0,1\}$ and each small simplex s is contained in some edge, say e. The coefficient α_s depends on the integrals over the small simplices of e: if x is the vector of these integrals with the chosen indexing, α_s is the dot product of x and the ith row of A^{-1}, where i is the index of s in e. Notice that the coefficients of those small nodes that are contained in two edges only depend on the value at the node itself; see rows 1 and 3 of A_n^{-1}. This ensures that the coefficients are well-defined, as was predicted in Section 3.5.

At any point q, most of the functions in the sum $\sum_s \alpha_s w^s$ are zero; in fact, only those w^s whose small simplex s is contained in the same edge as q can be nonzero at q. In practice we wish to evaluate the approximation at point q, and for this the expression $\sum_s \alpha_s w^s$ is not needed.

It's more practical to consider only those forms that matter. This strategy to approximate a 0-form ω at a point q is formulated in following algorithm:

Algorithm 1 Approximating 0-forms in one dimension.

1. Find the edge e containing q.
2. Compute the coefficient vector $a = (a_1, a_2, a_3)^T = A_n^{-1}x$, where $x = (x_1, x_2, x_3)^T$ contains the values of ω at the small nodes of e, with the chosen indexing.
3. The approximation is $a_1 w^1(q) + a_2 w^2(q) + a_3 w^3(q)$, where the forms w^i correspond to the small nodes of e with the chosen indexing.

The algorithm for 1-forms is similar, but we list it for the sake of completeness. If ω is a 1-form, it can be approximated at q as follows:

Algorithm 2 Approximating 1-forms in one dimension.

1. Find the edge e containing q.
2. Compute the coefficient vector $a = (a_1, a_2)^T = A_e^{-1}x$, where $x = (x_1, x_2)^T$ contains the integrals of ω over the small edges of e, with the chosen indexing.
3. The approximation is $a_1 w^1(q) + a_2 w^2(q)$, where the forms w^i correspond to the small edges of e with the chosen indexing.

The idea of the higher order approximations is very easy to see in the one-dimensional case. To illustrate this, we consider the 0-form $\omega(x) = \sin(x)\cos(x)$ in the interval $[0,3]$ and a mesh with five evenly spaced nodes $x_1, \ldots, x_5$. This means that there are four edges of length 0.75. Approximating ω with lowest order Whitney forms is simply connecting the points $(x_i, \omega(x_i))$ with straight line segments (see Figure 8).

In other words, for each edge $[x_i, x_{i+1}]$, the approximation is the linear function that coincides with ω at the endpoints. Suppose now that the nodes x_2 and x_4 are considered small simplices. Then we have two edges, $[x_1, x_3]$ and $[x_3, x_5]$, both of length 1.5, and a small node at each midedge. On both edges, we can approximate ω with the quadratic function that coincides with ω at the endpoints and the midpoint (see Figure 9). This is exactly the approximation obtained with second order Whitney forms using Algorithm 1.

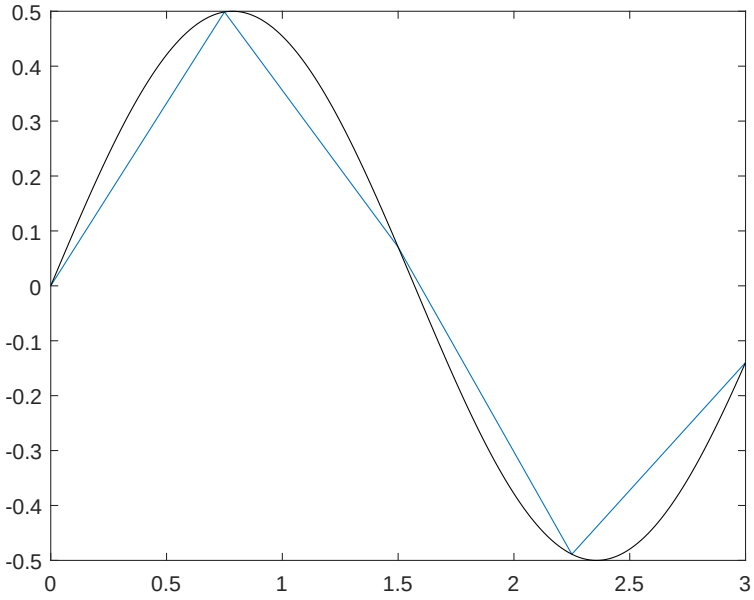

Figure 8. Approximating the 0-form $\omega(x) = \sin(x)\cos(x)$ in the interval $[0,3]$ using lowest order Whitney forms and a mesh with five evenly spaced nodes. The function ω is in black and the resulting approximation in blue.

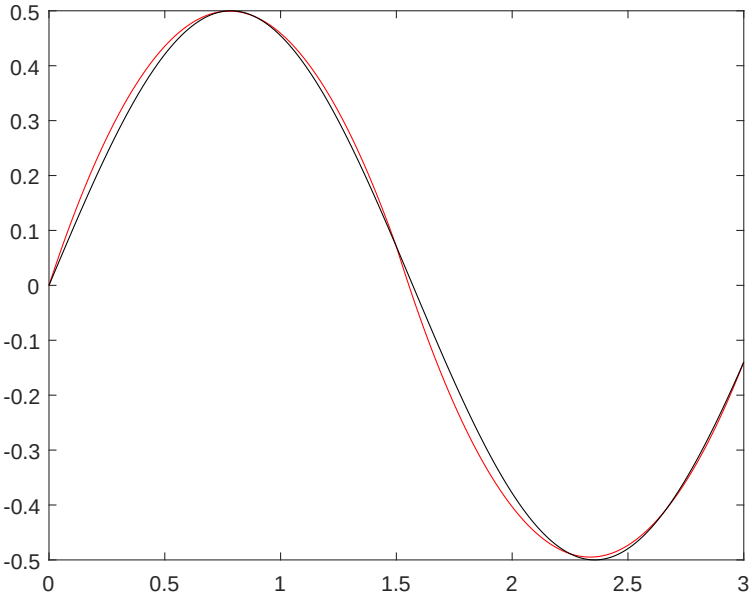

Figure 9. Approximating ω using second order Whitney forms. The function ω is in black and the resulting approximation in red. Compare to Figure 8: the two nodes at $x = 0.75$ and $x = 2.25$ are now considered small nodes, so we get quadratic approximations on the two edges $[0,1.5]$ and $[1.5,3]$.

This shows the idea: two adjacent edges are considered as one big edge, and then we automatically have the small simplices needed to use second order Whitney forms. To generalise this to higher dimensions we have to build the mesh such that the small simplices are a part of it, but the basic idea is still the same.

5.2 Two-dimensional case

In two dimensions we have facets, edges, and nodes. Consider the small simplices of the facet $f = mnl$. There are 9 small nodes, 9 small edges, and 3 small facets (recall Figure 3, left). We will again indentify the two small nodes at each midedge that are exactly the same, which leaves us with 6 small nodes. For small edges, (3.3) shows that the forms $\lambda_l w^{mn}$, $\lambda_m w^{nl}$, and $\lambda_n w^{lm}$ are linearly dependent. We drop $\lambda_m w^{nl}$ and choose the following indexing and orientations for the small simplices (Table 3):

Small nodes		
$\{m,m\} \leftarrow 1$	~~$\{n,m\}$~~	~~$\{l,m\}$~~
$\{m,n\} \leftarrow 2$	$\{n,n\} \leftarrow 4$	~~$\{l,n\}$~~
$\{m,l\} \leftarrow 3$	$\{n,l\} \leftarrow 5$	$\{l,l\} \leftarrow 6$

Small edges		
$\{m,mn\} \leftarrow 1$	$\{n,mn\} \leftarrow 3$	$\{l,mn\} \leftarrow 6$
~~$\{m,nl\}$~~	$\{n,nl\} \leftarrow 4$	$\{l,nl\} \leftarrow 7$
$\{m,lm\} \leftarrow 2$	$\{n,lm\} \leftarrow 5$	$\{l,lm\} \leftarrow 8$

Small facets		
$\{m,f\} \leftarrow 1$	$\{n,f\} \leftarrow 2$	$\{l,f\} \leftarrow 3$

Table 3. Indexing of the small simplices of the facet $f = mnl$.

Next we compute the matrices A whose elements A_{ij} are given as $A_{ij} = \int_{s_i} w^j$. Now there are three of them: A_n for small nodes, A_e for small edges, and A_f for small facets. A_n and its inverse are easily computed:

$$A_n = \frac{1}{4}\begin{bmatrix} 4 & 0 & 0 & 0 & 0 & 0 \\ 1 & 1 & 0 & 1 & 0 & 0 \\ 1 & 0 & 1 & 0 & 0 & 1 \\ 0 & 0 & 0 & 4 & 0 & 0 \\ 0 & 0 & 0 & 1 & 1 & 1 \\ 0 & 0 & 0 & 0 & 0 & 4 \end{bmatrix}, \quad A_n^{-1} = \begin{bmatrix} 1 & 0 & 0 & 0 & 0 & 0 \\ -1 & 4 & 0 & -1 & 0 & 0 \\ -1 & 0 & 4 & 0 & 0 & -1 \\ 0 & 0 & 0 & 1 & 0 & 0 \\ 0 & 0 & 0 & -1 & 4 & -1 \\ 0 & 0 & 0 & 0 & 0 & 1 \end{bmatrix}.$$

For A_e we need to compute the integrals over small edges. First notice that the tangential component of $\nabla\lambda_i$ on the edge $e = jk$ is $1/|e|$ if $i = k$, $-1/|e|$ if $i = j$, and 0 if $i \notin jk$ (see Figure 10). Consequently, since the small edges are parallel to the big edges, the tangential components of the lowest order Whitney 1-forms are actually constant on each small edge. This is because λ_{f-e} and $\lambda_j + \lambda_k$ are constant on small edges parallel to the big edge $e = jk$.

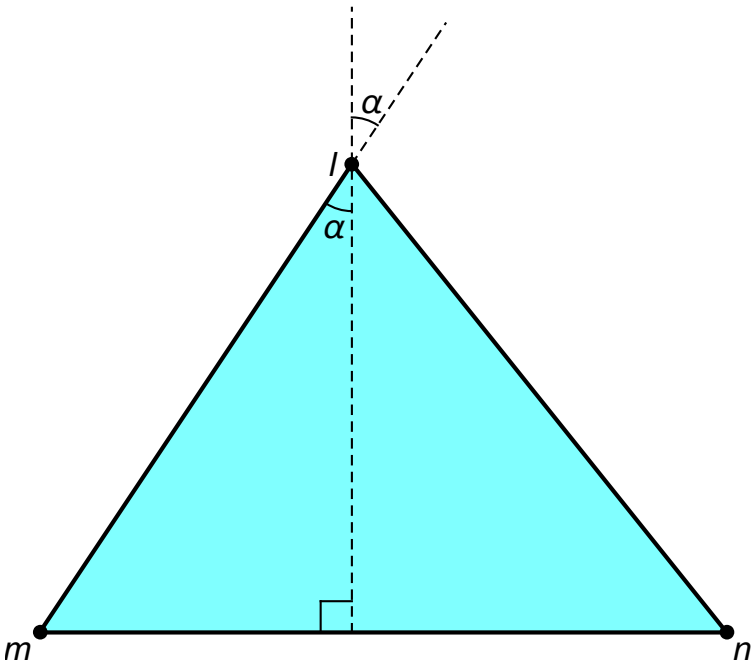

Figure 10. $\nabla\lambda_l$ is the vector parallel to the altitude through the node l and has length $\frac{1}{h_l}$, where h_l is the height with respect to l. Its tangential component on the edge ml is $\cos(\alpha)\,\|\nabla\lambda_l\| = \frac{h_l}{|ml|}\cdot\frac{1}{h_l} = \frac{1}{|ml|}$.

Therefore, the integral of the form $w^{\{i,e\}}$ over the small edge s can be written as the product $\int_s \lambda_i w^e = \frac{1}{|s|}(\int_s \lambda_i)(\int_s w^e)$, and A_e can now be constructed easily: we only need to integrate the lowest order Whitney forms and the barycentric functions over the small edges. To illustrate the discussion above, let's compute some of the integrals as an example.

Example Let's determine $(A_e)_4^5 = \int_{s_5} w^4 = \int_{s_5} w^{\{n,nl\}} = \int_{s_5} \lambda_n(\lambda_n \nabla\lambda_l - \lambda_l \nabla\lambda_n)\cdot t_5$, where by t_5 we denote the unit tangent vector of the small edge s_5. s_5 is parallel to lm, so the tangential components of $\nabla\lambda_l$ and $\nabla\lambda_n$ are $\nabla\lambda_l \cdot t_5 = -1/|lm| = -1/(2|s_5|)$ and $\nabla\lambda_n \cdot t_5 = 0$ on s_5. In addition, $\lambda_n = 1/2$ on s_5. We get

$$\int_{s_5} \lambda_n(\lambda_n \nabla\lambda_l - \lambda_l \nabla\lambda_n)\cdot t_5 = \int_{s_5} \lambda_n\left(-\frac{1}{2}\cdot\frac{1}{2|s_5|}\right) = -\frac{1}{4|s_5|}\int_{s_5}\lambda_n = -\frac{1}{4|s_5|}\cdot\frac{|s_5|}{2} = -\frac{1}{8}.$$

$(A_e)_2^5$ and $(A_e)_7^5$ are computed similarly:

$$(A_e)_2^5 = \int_{s_5} \lambda_m(\lambda_n \nabla\lambda_l - \lambda_l \nabla\lambda_n)\cdot t_5 = -\frac{1}{4|s_5|}\int_{s_5}\lambda_m = -\frac{1}{4|s_5|}\cdot\frac{|s_5|}{4} = -\frac{1}{16},$$
$$(A_e)_7^5 = \int_{s_5} \lambda_l(\lambda_n \nabla\lambda_l - \lambda_l \nabla\lambda_n)\cdot t_5 = -\frac{1}{4|s_5|}\int_{s_5}\lambda_l = -\frac{1}{4|s_5|}\cdot\frac{|s_5|}{4} = -\frac{1}{16}.$$

The matrix A_f is easily computed: the proxy field of the lowest order Whitney 2-form w^f is $\star w^f = 1/|f|$, and we only have to integrate barycentric functions over the small facets. The matrices A_e and A_f and their inverses read

$$A_e = \frac{1}{16}\begin{bmatrix} 6 & 0 & 2 & 0 & 0 & 0 & 0 & 0 \\ 0 & 6 & 0 & 0 & 0 & 0 & 0 & 2 \\ 2 & 0 & 6 & 0 & 0 & 0 & 0 & 0 \\ 0 & 0 & 0 & 6 & 0 & 0 & 2 & 0 \\ -1 & 1 & -2 & -2 & 2 & -1 & -1 & 1 \\ 1 & -1 & 1 & -1 & -1 & 2 & -2 & -2 \\ 0 & 0 & 0 & 2 & 0 & 0 & 6 & 0 \\ 0 & 2 & 0 & 0 & 0 & 0 & 0 & 6 \end{bmatrix}, \quad A_f = \frac{1}{24}\begin{bmatrix} 4 & 1 & 1 \\ 1 & 4 & 1 \\ 1 & 1 & 4 \end{bmatrix},$$

$$A_e^{-1} = \frac{1}{3}\begin{bmatrix} 9 & 0 & -3 & 0 & 0 & 0 & 0 & 0 \\ 0 & 9 & 0 & 0 & 0 & 0 & 0 & -3 \\ -3 & 0 & 9 & 0 & 0 & 0 & 0 & 0 \\ 0 & 0 & 0 & 9 & 0 & 0 & -3 & 0 \\ 0 & -3 & 8 & 11 & 32 & 16 & 7 & 1 \\ -3 & 0 & 1 & 7 & 16 & 32 & 11 & 8 \\ 0 & 0 & 0 & -3 & 0 & 0 & 9 & 0 \\ 0 & -3 & 0 & 0 & 0 & 0 & 0 & 9 \end{bmatrix}, \quad A_f^{-1} = \frac{4}{3}\begin{bmatrix} 5 & -1 & -1 \\ -1 & 5 & -1 \\ -1 & -1 & 5 \end{bmatrix}.$$

The procedure for approximating p-forms is similar as in the one-dimensional case. Again, the matrices A_n^{-1} and A_e^{-1} illustrate why the coefficients are well-defined. The coefficients of small nodes at midedges depend only on the small nodes of that edge, and the coefficients of small nodes that match with big nodes depend only on the node itself. The coefficients of small edges that are part of a big edge depend only on the two small edges of that big edge.

As before, at any point most of the basis functions are zero, and in practice we don't write the approximation in terms of the basis functions. The following algorithms for $p \in \{0,1,2\}$ show how the approximation of a p-form ω is evaluated at any point q.

Algorithm 3 Approximating 0-forms in two dimensions.

1. Find the facet f containing q.
2. Compute the coefficient vector $a = (a_1, \ldots, a_6)^T = A_n^{-1}x$, where $x = (x_1, \ldots, x_6)^T$ contains the values of ω at the small nodes of f.
3. The approximation is $a_1 w^1(q) + \ldots + a_6 w^6(q)$, where the forms w^i correspond to the small nodes of f.

Algorithm 4 Approximating 1-forms in two dimensions.

1. Find the facet f containing q.
2. Compute the coefficient vector $a = (a_1, \ldots, a_8)^T = A_e^{-1}x$, where $x = (x_1, \ldots, x_8)^T$ contains the integrals of ω over the small edges of f.
3. The approximation is $a_1 w^1(q) + \ldots + a_8 w^8(q)$, where the forms w^i correspond to the small edges of f.

Algorithm 5 Approximating 2-forms in two dimensions.

1. Find the facet f containing q.
2. Compute the coefficient vector $a = (a_1, a_2, a_3)^T = A_f^{-1} x$, where $x = (x_1, x_2, x_3)^T$ contains the integrals of ω over the small facets of f.
3. The approximation is $a_1 w^1(q) + a_2 w^2(q) + a_3 w^3(q)$, where the forms w^i correspond to the small facets of f.

In the two-dimensional case it's possible to provide illustrating examples with pictures. Vector fields can be visualised by converting the value (x, y) to RGB colour $(128 + 128x, 128 + 128y, 128)$ and then making sure that the colour values are between 0 and 255. In the following example we consider the domain $D = [-1, 1] \times [-1, 1]$ and a mesh consisting of triangles that cover D. We refine the mesh and integrate a test function over the small edges. In this case the refined mesh is simplicial, so we can approximate the test function with either lowest order Whitney forms in the refined mesh or second order Whitney forms using the small simplices. These two approximations are compared with the initial function.

In Figure 11 we have a picture of the vector field $g(x, y) = (\sin(5x), \sin(5y)\cos(5x))$. Recall that g can be identified with the 1-form $\flat g$ whose proxy field g is. To approximate g, we start with a two-dimensional simplicial mesh whose triangles are then divided into small simplices. The integration of g over the small edges is performed numerically. The mesh grain h in this example means that the initial mesh consists of isosceles triangles with base and height h. Recall that with lowest order Whitney forms we use the refined mesh, whose grain actually is $\frac{h}{2}$, since the displayed values for h are always with respect to the initial mesh. The approximations given by $h = 1.0$ are shown in Figure 12.

We estimated numerically the L^2 norm $\|\cdot\|_2$ of the error $g_a - g$, where g_a denotes the approximation of g. This was done using a quadrature rule with four points per triangle (Dunavant 1985). In the case $h = 1.0$, with lowest order Whitney forms we have $\|g_a - g\|_2 \approx 1.13797$ and with second order approximations $\|g_a - g\|_2 \approx 1.07132$. This mesh was rather coarse so the approximations are inaccurate, but the accuracy of the approximations increases when the mesh grain h decreases. For comparison, see Figures 13 and 14, which display the approximations given by $h = 0.25$ and $h = 0.125$.

Figure 11. The vector field $g(x,y) = (\sin(5x), \sin(5y)\cos(5x))$ in the domain $D = [-1,1]^2$.

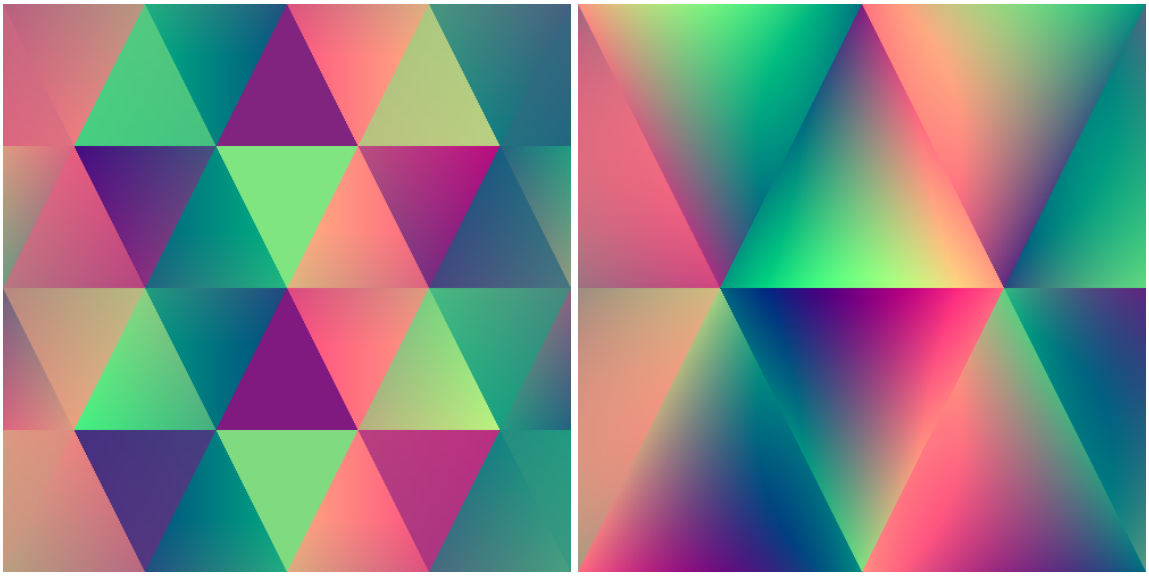

Figure 12. Approximating g with lowest order Whitney forms (left) and second order Whitney forms (right) when $h = 1.0$.

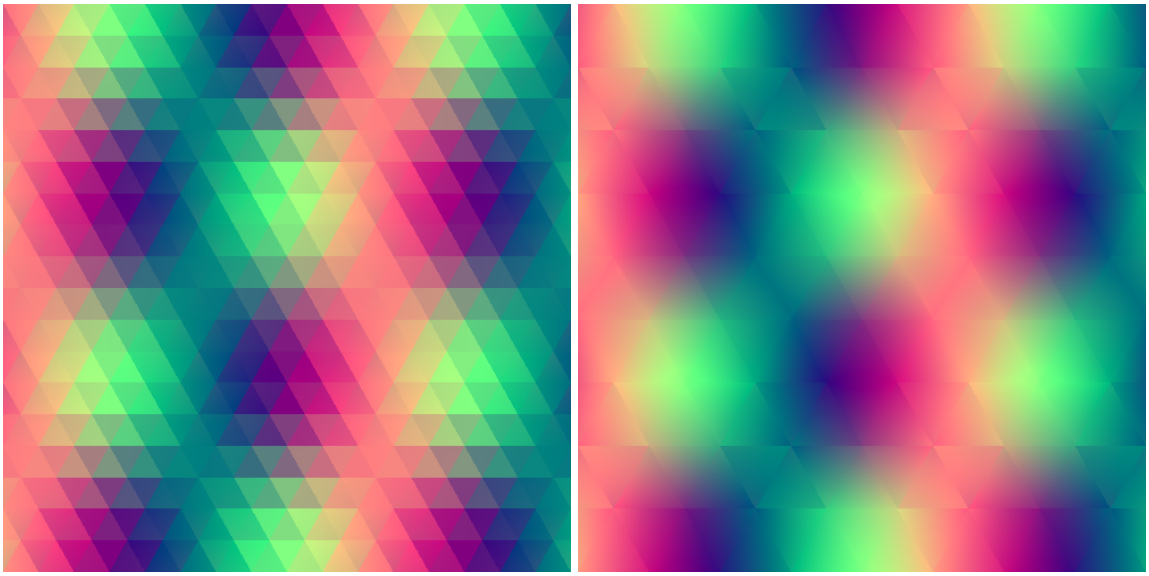

Figure 13. Approximating g with lowest order Whitney forms (left) and second order Whitney forms (right) when $h = 0.25$.

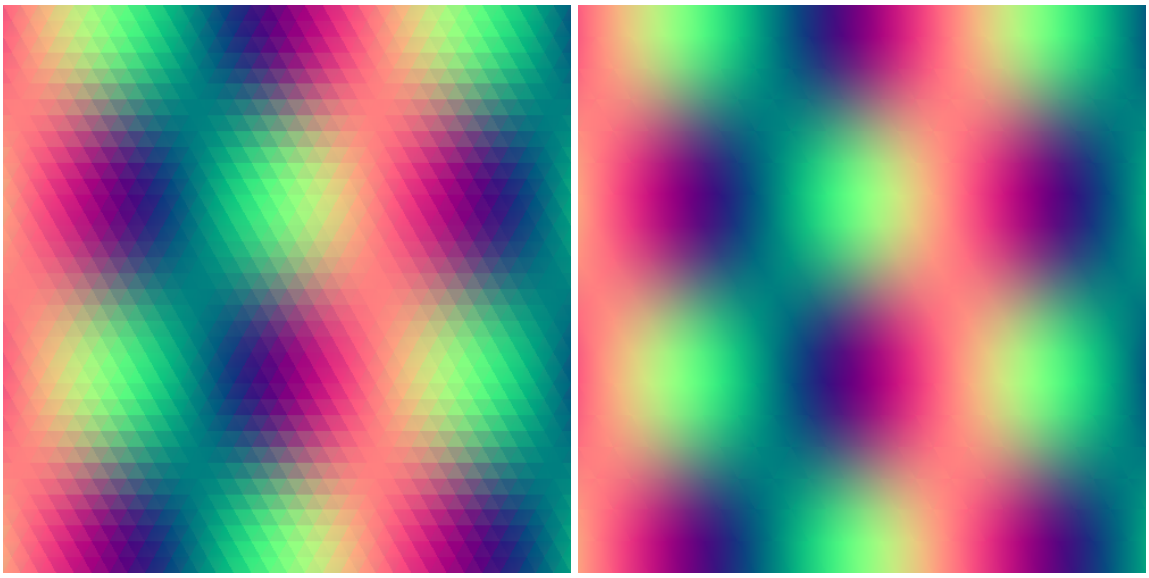

Figure 14. Approximating g with lowest order Whitney forms (left) and second order Whitney forms (right) when $h = 0.125$.

To study the convergence we have computed the error norm for different values of h. The results are shown in Table 4.

Mesh grain h	0.125	0.25	0.50	1.0
Error norm, lowest order Whitney 1-forms	0.152457	0.303902	0.58955	1.13797
Error norm, second order Whitney 1-forms	0.022847	0.090019	0.31886	1.07132

Table 4. L^2 norm of the error and its dependence on the mesh grain h when approximating g with lowest and second order Whitney forms.

The results indicate that to halve the error we have to halve the mesh grain when using lowest order Whitney forms, but with second order forms a better convergence rate is achieved. We have also plotted the results in Figure 15. The error norm is plotted against $\log_2\left(\frac{1}{h}\right)$, which in our case gets the values 0, 1, 2, and 3. Using a logarithmic scale for the error norm, the data points are aligned in straight lines.

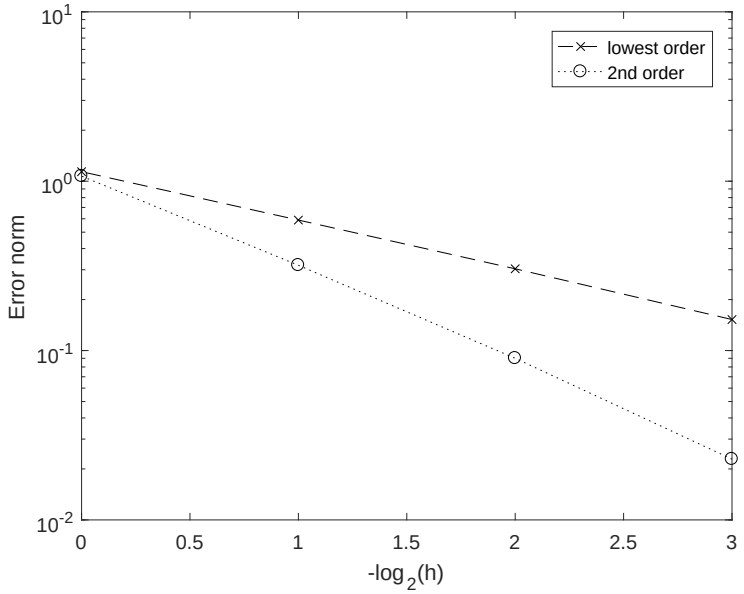

Figure 15. Visualisation of the results displayed in Table 4.

5.3 Three-dimensional case

Consider a three-dimensional mesh and the small simplices of a volume $v = mnlk$. There are 16 small nodes, 24 small edges, 16 small facets, and 4 small volumes (recall Figure 4, left).

Identifying the two small nodes at each midedge as before leaves us with 10 small nodes. By (3.3), we have three linearly dependent forms for each of the four facets of v. The following sets are linearly dependent:

$$\{\lambda_m w^{nl}, \lambda_n w^{lm}, \lambda_l w^{mn}\}, \{\lambda_m w^{nk}, \lambda_n w^{mk}, \lambda_k w^{mn}\}, \{\lambda_n w^{lk}, \lambda_l w^{nk}, \lambda_k w^{nl}\}, \{\lambda_l w^{mk}, \lambda_m w^{lk}, \lambda_k w^{lm}\}.$$

We drop the small simplices $\{m,nl\}$, $\{n,mk\}$, $\{l,nk\}$, and $\{k,lm\}$, which leaves us with 20 small edges. (3.3) also shows that the 2-forms $\lambda_m w^{nlk}$, $\lambda_n w^{lmk}$, $\lambda_l w^{mnk}$, and $\lambda_k w^{mnl}$ are linearly dependent. We drop $\lambda_m w^{nlk}$ and choose the following indexing and orientations for the small simplices (Table 5):

Small nodes			
$\{m,m\} \leftarrow 1$	~~$\{n,m\}$~~	~~$\{l,m\}$~~	~~$\{k,m\}$~~
$\{m,n\} \leftarrow 2$	$\{n,n\} \leftarrow 4$	~~$\{l,n\}$~~	~~$\{k,n\}$~~
$\{m,l\} \leftarrow 3$	$\{n,l\} \leftarrow 5$	$\{l,l\} \leftarrow 6$	~~$\{k,l\}$~~
$\{m,k\} \leftarrow 7$	$\{n,k\} \leftarrow 8$	$\{l,k\} \leftarrow 9$	$\{k,k\} \leftarrow 10$

Small edges			
$\{m,mn\} \leftarrow 1$	$\{n,mn\} \leftarrow 6$	$\{l,mn\} \leftarrow 11$	$\{k,mn\} \leftarrow 16$
~~$\{m,nl\}$~~	$\{n,nl\} \leftarrow 7$	$\{l,nl\} \leftarrow 12$	$\{k,nl\} \leftarrow 17$
$\{m,lm\} \leftarrow 2$	$\{n,lm\} \leftarrow 8$	$\{l,lm\} \leftarrow 13$	~~$\{k,lm\}$~~
$\{m,mk\} \leftarrow 3$	~~$\{n,mk\}$~~	$\{l,mk\} \leftarrow 14$	$\{k,mk\} \leftarrow 18$
$\{m,nk\} \leftarrow 4$	$\{n,nk\} \leftarrow 9$	~~$\{l,nk\}$~~	$\{k,nk\} \leftarrow 19$
$\{m,lk\} \leftarrow 5$	$\{n,lk\} \leftarrow 10$	$\{l,lk\} \leftarrow 15$	$\{k,lk\} \leftarrow 20$

Small facets			
$\{m,mnl\} \leftarrow 1$	$\{n,mnl\} \leftarrow 4$	$\{l,mnl\} \leftarrow 8$	$\{k,mnl\} \leftarrow 12$
$\{m,mnk\} \leftarrow 2$	$\{n,mnk\} \leftarrow 5$	$\{l,mnk\} \leftarrow 9$	$\{k,mnk\} \leftarrow 13$
~~$\{m,nlk\}$~~	$\{n,nlk\} \leftarrow 6$	$\{l,nlk\} \leftarrow 10$	$\{k,nlk\} \leftarrow 14$
$\{m,lmk\} \leftarrow 3$	$\{n,lmk\} \leftarrow 7$	$\{l,lmk\} \leftarrow 11$	$\{k,lmk\} \leftarrow 15$

Small volumes			
$\{m,v\} \leftarrow 1$	$\{n,v\} \leftarrow 2$	$\{l,v\} \leftarrow 3$	$\{k,v\} \leftarrow 4$

Table 5. Indexing of the small simplices of the volume $v = mnlk$.

The algorithms for approximating p-forms are similar as in lower dimensions. For these we

again need the matrices A whose elements A_{ij} are given as $A_{ij} = \int_{s_i} w^j$. Let's denote these by A_n for small nodes, A_e for small edges, A_f for small facets, and A_v for small volumes, and consider how they are computed.

The matrix A_n and its inverse are easily computed and they read

$$A_n = \frac{1}{4}\begin{bmatrix} 4 & 0 & 0 & 0 & 0 & 0 & 0 & 0 & 0 & 0 \\ 1 & 1 & 0 & 1 & 0 & 0 & 0 & 0 & 0 & 0 \\ 1 & 0 & 1 & 0 & 0 & 1 & 0 & 0 & 0 & 0 \\ 0 & 0 & 0 & 4 & 0 & 0 & 0 & 0 & 0 & 0 \\ 0 & 0 & 0 & 1 & 1 & 1 & 0 & 0 & 0 & 0 \\ 0 & 0 & 0 & 0 & 0 & 4 & 0 & 0 & 0 & 0 \\ 1 & 0 & 0 & 0 & 0 & 0 & 1 & 0 & 0 & 1 \\ 0 & 0 & 0 & 1 & 0 & 0 & 0 & 1 & 0 & 1 \\ 0 & 0 & 0 & 0 & 0 & 1 & 0 & 0 & 1 & 1 \\ 0 & 0 & 0 & 0 & 0 & 0 & 0 & 0 & 0 & 4 \end{bmatrix}, A_n^{-1} = \begin{bmatrix} 1 & 0 & 0 & 0 & 0 & 0 & 0 & 0 & 0 & 0 \\ -1 & 4 & 0 & -1 & 0 & 0 & 0 & 0 & 0 & 0 \\ -1 & 0 & 4 & 0 & 0 & -1 & 0 & 0 & 0 & 0 \\ 0 & 0 & 0 & 1 & 0 & 0 & 0 & 0 & 0 & 0 \\ 0 & 0 & 0 & -1 & 4 & -1 & 0 & 0 & 0 & 0 \\ 0 & 0 & 0 & 0 & 0 & 1 & 0 & 0 & 0 & 0 \\ -1 & 0 & 0 & 0 & 0 & 0 & 4 & 0 & 0 & -1 \\ 0 & 0 & 0 & -1 & 0 & 0 & 0 & 4 & 0 & -1 \\ 0 & 0 & 0 & 0 & 0 & -1 & 0 & 0 & 4 & -1 \\ 0 & 0 & 0 & 0 & 0 & 0 & 0 & 0 & 0 & 1 \end{bmatrix}.$$

For A_e we must compute the integrals over small edges. This is possible when we make similar observations as in two dimensions. First, the tangential component of $\nabla\lambda_i$ on the edge $e = jk$ is $1/|e|$ if $i = k$, $-1/|e|$ if $i = j$, and 0 if $i \notin jk$ (see Figure 16). Consequently, since the small edges are parallel to the big edges, the tangential components of the lowest order Whitney 1-forms are constant on each small edge. This is because $\lambda_j + \lambda_k$ is constant on small edges parallel to the big edge jk and λ_j is constant on small edges parallel to big edges that don't contain j.

Therefore, we can again write the integral of the form $w^{\{i,e\}}$ over the small edge s as the product $\int_s \lambda_i w^e = \frac{1}{|s|}(\int_s \lambda_i)(\int_s w^e)$, so once we know the integrals of the lowest order Whitney forms and the barycentric functions over the small edges, A_e can be constructed from these.

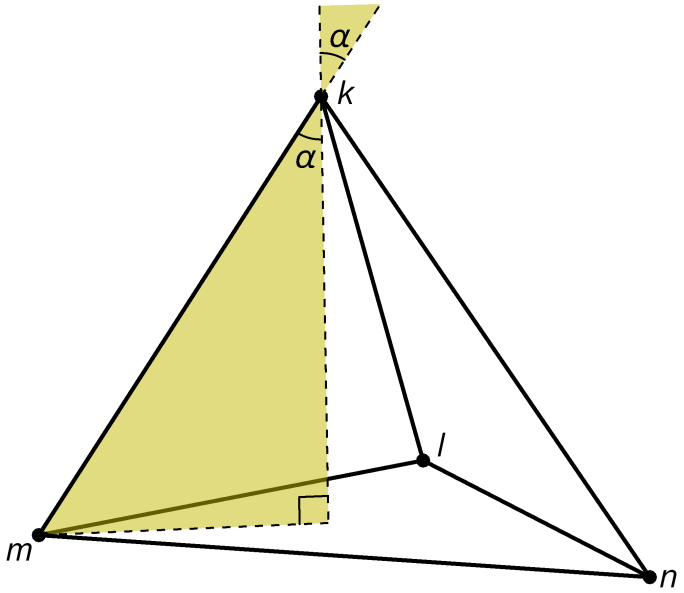

Figure 16. $\nabla\lambda_k$ is the vector normal to the facet mnl and has length $\frac{1}{h_k}$, where h_k is the height with respect to the node k. Its tangential component on the edge mk is $\cos(\alpha)\,\|\nabla\lambda_k\| = \frac{h_k}{|mk|}\cdot\frac{1}{h_k} = \frac{1}{|mk|}$.

With our choice of indexing, the matrix A_e and its inverse are

$$A_e = \frac{1}{16}\begin{bmatrix}
6 & 0 & 0 & 0 & 0 & 2 & 0 & 0 & 0 & 0 & 0 & 0 & 0 & 0 & 0 & 0 & 0 & 0 & 0 & 0\\
0 & 6 & 0 & 0 & 0 & 0 & 0 & 0 & 0 & 0 & 0 & 0 & 2 & 0 & 0 & 0 & 0 & 0 & 0 & 0\\
0 & 0 & 6 & 0 & 0 & 0 & 0 & 0 & 0 & 0 & 0 & 0 & 0 & 0 & 0 & 0 & 0 & 2 & 0 & 0\\
-2 & 0 & 2 & 2 & 0 & -1 & 0 & 0 & 1 & 0 & 0 & 0 & 0 & 0 & 0 & -1 & 0 & 1 & 1 & 0\\
0 & 2 & 2 & 0 & 2 & 0 & 0 & 0 & 0 & 0 & 0 & 0 & 1 & 1 & 1 & 0 & 0 & 1 & 0 & 1\\
2 & 0 & 0 & 0 & 0 & 6 & 0 & 0 & 0 & 0 & 0 & 0 & 0 & 0 & 0 & 0 & 0 & 0 & 0 & 0\\
0 & 0 & 0 & 0 & 0 & 0 & 6 & 0 & 0 & 0 & 0 & 2 & 0 & 0 & 0 & 0 & 0 & 0 & 0 & 0\\
-1 & 1 & 0 & 0 & 0 & -2 & -2 & 2 & 0 & 0 & -1 & -1 & 1 & 0 & 0 & 0 & 0 & 0 & 0 & 0\\
0 & 0 & 0 & 0 & 0 & 0 & 0 & 0 & 6 & 0 & 0 & 0 & 0 & 0 & 0 & 0 & 0 & 0 & 2 & 0\\
0 & 0 & 0 & 0 & 0 & 0 & -2 & 0 & 2 & 2 & 0 & -1 & 0 & 0 & 1 & 0 & -1 & 0 & 1 & 1\\
1 & -1 & 0 & 0 & 0 & 1 & -1 & -1 & 0 & 0 & 2 & -2 & -2 & 0 & 0 & 0 & 0 & 0 & 0 & 0\\
0 & 0 & 0 & 0 & 0 & 0 & 2 & 0 & 0 & 0 & 0 & 6 & 0 & 0 & 0 & 0 & 0 & 0 & 0 & 0\\
0 & 2 & 0 & 0 & 0 & 0 & 0 & 0 & 0 & 0 & 0 & 0 & 6 & 0 & 0 & 0 & 0 & 0 & 0 & 0\\
0 & -1 & 1 & 0 & 1 & 0 & 0 & 0 & 0 & 0 & 0 & 0 & -2 & 2 & 2 & 0 & 0 & 1 & 0 & 1\\
0 & 0 & 0 & 0 & 0 & 0 & 0 & 0 & 0 & 0 & 0 & 0 & 0 & 0 & 6 & 0 & 0 & 0 & 0 & 2\\
1 & 0 & 1 & -1 & 0 & 1 & 0 & 0 & -1 & 0 & 0 & 0 & 0 & 0 & 0 & 2 & 0 & 2 & -2 & 0\\
0 & 0 & 0 & 0 & 0 & 0 & 1 & 0 & 1 & -1 & 0 & 1 & 0 & 0 & -1 & 0 & 2 & 0 & 2 & -2\\
0 & 0 & 2 & 0 & 0 & 0 & 0 & 0 & 0 & 0 & 0 & 0 & 0 & 0 & 0 & 0 & 0 & 6 & 0 & 0\\
0 & 0 & 0 & 0 & 0 & 0 & 0 & 0 & 2 & 0 & 0 & 0 & 0 & 0 & 0 & 0 & 0 & 0 & 6 & 0\\
0 & 0 & 0 & 0 & 0 & 0 & 0 & 0 & 0 & 0 & 0 & 0 & 0 & 0 & 2 & 0 & 0 & 0 & 0 & 6
\end{bmatrix},$$

$$A_e^{-1} = \frac{1}{3}\begin{bmatrix}
9 & 0 & 0 & 0 & 0 & -3 & 0 & 0 & 0 & 0 & 0 & 0 & 0 & 0 & 0 & 0 & 0 & 0 & 0 & 0 \\
0 & 9 & 0 & 0 & 0 & 0 & 0 & 0 & 0 & 0 & 0 & 0 & -3 & 0 & 0 & 0 & 0 & 0 & 0 & 0 \\
0 & 0 & 9 & 0 & 0 & 0 & 0 & 0 & 0 & 0 & 0 & 0 & 0 & 0 & 0 & 0 & 0 & -3 & 0 & 0 \\
8 & 0 & -11 & 32 & 0 & 0 & 0 & 0 & -3 & 0 & 0 & 0 & 0 & 0 & 0 & 16 & 0 & -7 & 1 & 0 \\
0 & -11 & -8 & 0 & 32 & 0 & 0 & 0 & 0 & 0 & 0 & 0 & -7 & -16 & 1 & 0 & 0 & 0 & 0 & -3 \\
-3 & 0 & 0 & 0 & 0 & 9 & 0 & 0 & 0 & 0 & 0 & 0 & 0 & 0 & 0 & 0 & 0 & 0 & 0 & 0 \\
0 & 0 & 0 & 0 & 0 & 0 & 9 & 0 & 0 & 0 & 0 & -3 & 0 & 0 & 0 & 0 & 0 & 0 & 0 & 0 \\
0 & -3 & 0 & 0 & 0 & 8 & 11 & 32 & 0 & 0 & 16 & 7 & 1 & 0 & 0 & 0 & 0 & 0 & 0 & 0 \\
0 & 0 & 0 & 0 & 0 & 0 & 0 & 0 & 9 & 0 & 0 & 0 & 0 & 0 & 0 & 0 & 0 & -3 & 0 & \\
0 & 0 & 0 & 0 & 0 & 0 & 8 & 0 & -11 & 32 & 0 & 0 & 0 & 0 & -3 & 0 & 16 & 0 & -7 & 1 \\
-3 & 0 & 0 & 0 & 0 & 1 & 7 & 16 & 0 & 0 & 32 & 11 & 8 & 0 & 0 & 0 & 0 & 0 & 0 & 0 \\
0 & 0 & 0 & 0 & 0 & 0 & -3 & 0 & 0 & 0 & 0 & 9 & 0 & 0 & 0 & 0 & 0 & 0 & 0 & 0 \\
0 & -3 & 0 & 0 & 0 & 0 & 0 & 0 & 0 & 0 & 0 & 0 & 9 & 0 & 0 & 0 & 0 & 0 & 0 & 0 \\
0 & 7 & 1 & 0 & -16 & 0 & 0 & 0 & 0 & 0 & 0 & 0 & 11 & 32 & -8 & 0 & 0 & -3 & 0 & 0 \\
0 & 0 & 0 & 0 & 0 & 0 & 0 & 0 & 0 & 0 & 0 & 0 & 0 & 0 & 9 & 0 & 0 & 0 & 0 & -3 \\
1 & 0 & -7 & 16 & 0 & -3 & 0 & 0 & 0 & 0 & 0 & 0 & 0 & 0 & 0 & 32 & 0 & -11 & 8 & 0 \\
0 & 0 & 0 & 0 & 0 & 0 & 1 & 0 & -7 & 16 & 0 & -3 & 0 & 0 & 0 & 0 & 32 & 0 & -11 & 8 \\
0 & 0 & -3 & 0 & 0 & 0 & 0 & 0 & 0 & 0 & 0 & 0 & 0 & 0 & 0 & 0 & 0 & 9 & 0 & 0 \\
0 & 0 & 0 & 0 & 0 & 0 & 0 & 0 & -3 & 0 & 0 & 0 & 0 & 0 & 0 & 0 & 0 & 0 & 9 & 0 \\
0 & 0 & 0 & 0 & 0 & 0 & 0 & 0 & 0 & 0 & 0 & 0 & 0 & 0 & -3 & 0 & 0 & 0 & 0 & 9
\end{bmatrix}.$$

Next, consider the computation of A_f, i.e. the integrals over the small facets of a tetrahedron $v = mnlk$. Recall that the proxy field of the Whitney 2-form w^f corresponding to the facet $f = lmn$ is

$$\sharp \star w^f = 2(\lambda_l \nabla\lambda_m \times \nabla\lambda_n + \lambda_m \nabla\lambda_n \times \nabla\lambda_l + \lambda_n \nabla\lambda_l \times \nabla\lambda_m).$$

$\nabla\lambda_i \times \nabla\lambda_j$ is orthogonal to both $\nabla\lambda_i$ and $\nabla\lambda_j$, so it is parallel to the edge e that is opposite to the edge ij. It can be shown that its length is $\frac{|e|}{6|v|}$. The normal component of $\nabla\lambda_i \times \nabla\lambda_j$ is zero on the facets that don't contain ij. On a facet f that contains ij, it is $\pm\frac{h}{6|v|}$, where h is the height of the tetrahedron v with respect to the facet f and the sign depends on whether the orientations of ij and f agree or not. Note that this doesn't depend on the ambient orientation: if it is changed, cross products change sign, but so do normal vectors, and the two changes of sign cancel each other.

Since the small facets are parallel to the big facets, these observations imply that the normal components of the lowest order Whitney 2-forms are actually constant on each small facet. This is because $\lambda_l + \lambda_m + \lambda_n$ is constant on small faces parallel to lmn and λ_i is constant on small facets parallel to the facet opposite to i. Therefore, the integral of the form $w^{\{i,f\}}$ over

the small facet s can be written as the product $\int_s \lambda_i w^f = \frac{1}{|s|}(\int_s \lambda_i)(\int_s w^f)$, and to construct A_f it suffices to integrate the lowest order Whitney forms and the barycentric functions over the small facets. The computation of the integrals is illustrated in the following example.

Example Let's determine $(A_f)_2^7$, i.e. the integral

$$\int_{s_7} w^2 = \int_{s_7} w^{\{m,mnk\}} = \int_{s_7} \lambda_m 2(\lambda_m \nabla\lambda_n \times \nabla\lambda_k + \lambda_n \nabla\lambda_k \times \nabla\lambda_m + \lambda_k \nabla\lambda_m \times \nabla\lambda_n) \cdot n_7,$$

where by n_7 we denote the unit normal vector of the small facet s_7. s_7 is parallel to the facet lmk, so the normal components of $\nabla\lambda_n \times \nabla\lambda_k$, $\nabla\lambda_k \times \nabla\lambda_m$, and $\nabla\lambda_m \times \nabla\lambda_n$ are

$$\nabla\lambda_n \times \nabla\lambda_k \cdot n_7 = 0, \nabla\lambda_k \times \nabla\lambda_m \cdot n_7 = -\frac{h}{6|v|}, \nabla\lambda_m \times \nabla\lambda_n \cdot n_7 = 0,$$

where h is the height of the tetrahedron with respect to the facet lmk. Thus,

$$(A_f)_2^7 = \int_{s_7} \lambda_m 2(\lambda_m \nabla\lambda_n \times \nabla\lambda_k + \lambda_n \nabla\lambda_k \times \nabla\lambda_m + \lambda_k \nabla\lambda_m \times \nabla\lambda_n) \cdot n_7 = \int_{s_7} 2\lambda_m \left(-\lambda_n \frac{h}{6|v|} \right)$$
$$= \int_{s_7} 2\lambda_m \left(-\frac{1}{2}\frac{h}{6|v|} \right) = -\frac{h}{6|v|} \int_{s_7} \lambda_m = -\frac{h}{6|v|} \cdot \frac{1}{6}|s_7| = -\frac{h}{6|v|} \cdot \frac{1}{6} \cdot \frac{3|v|}{4h} = -\frac{1}{48},$$

since the area of the facet lmk is $4|s_7|$ (so $|v| = \frac{4|s_7|h}{3}$) and $\lambda_n = 1/2$ on s_7. Similarly,

$$(A_f)_5^7 = -\frac{h}{6|v|} \int_{s_7} \lambda_n = -\frac{h}{6|v|} \cdot \frac{1}{2}|s_7| = -\frac{h}{6|v|} \cdot \frac{1}{2} \cdot \frac{3|v|}{4h} = -\frac{3}{48},$$
$$(A_f)_9^7 = -\frac{h}{6|v|} \int_{s_7} \lambda_l = -\frac{h}{6|v|} \cdot \frac{1}{6}|s_7| = -\frac{h}{6|v|} \cdot \frac{1}{6} \cdot \frac{3|v|}{4h} = -\frac{1}{48},$$
$$(A_f)_{13}^7 = -\frac{h}{6|v|} \int_{s_7} \lambda_k = -\frac{h}{6|v|} \cdot \frac{1}{6}|s_7| = -\frac{h}{6|v|} \cdot \frac{1}{6} \cdot \frac{3|v|}{4h} = -\frac{1}{48}.$$

The matrix A_f and its inverse read

$$A_f = \frac{1}{48}\begin{bmatrix}
8 & 0 & 0 & 2 & 0 & 0 & 0 & 2 & 0 & 0 & 0 & 0 & 0 & 0 & 0 \\
0 & 8 & 0 & 0 & 2 & 0 & 0 & 0 & 0 & 0 & 0 & 0 & 2 & 0 & 0 \\
0 & 0 & 8 & 0 & 0 & 0 & 0 & 0 & 0 & 0 & 2 & 0 & 0 & 0 & 2 \\
2 & 0 & 0 & 8 & 0 & 0 & 0 & 2 & 0 & 0 & 0 & 0 & 0 & 0 & 0 \\
0 & 2 & 0 & 0 & 8 & 0 & 0 & 0 & 0 & 0 & 0 & 0 & 2 & 0 & 0 \\
0 & 0 & 0 & 0 & 0 & 8 & 0 & 0 & 0 & 2 & 0 & 0 & 0 & 2 & 0 \\
1 & -1 & 1 & 3 & -3 & -3 & 3 & 1 & -1 & -1 & 1 & 1 & -1 & -1 & 1 \\
2 & 0 & 0 & 2 & 0 & 0 & 0 & 8 & 0 & 0 & 0 & 0 & 0 & 0 & 0 \\
1 & 1 & -1 & 1 & 1 & -1 & -1 & 3 & 3 & -3 & -3 & 1 & 1 & -1 & -1 \\
0 & 0 & 0 & 0 & 0 & 2 & 0 & 0 & 0 & 8 & 0 & 0 & 0 & 2 & 0 \\
0 & 0 & 2 & 0 & 0 & 0 & 0 & 0 & 0 & 0 & 8 & 0 & 0 & 0 & 2 \\
1 & 1 & 1 & 1 & 1 & 1 & 1 & 1 & 1 & 1 & 1 & 3 & 3 & 3 & 3 \\
0 & 2 & 0 & 0 & 2 & 0 & 0 & 0 & 0 & 0 & 0 & 0 & 8 & 0 & 0 \\
0 & 0 & 0 & 0 & 0 & 2 & 0 & 0 & 0 & 2 & 0 & 0 & 0 & 8 & 0 \\
0 & 0 & 2 & 0 & 0 & 0 & 0 & 0 & 0 & 0 & 2 & 0 & 0 & 0 & 8
\end{bmatrix},$$

$$A_f^{-1} = \frac{1}{3}\begin{bmatrix}
20 & 0 & 0 & -4 & 0 & 0 & 0 & -4 & 0 & 0 & 0 & 0 & 0 & 0 & 0 \\
0 & 20 & 0 & 0 & -4 & 0 & 0 & 0 & 0 & 0 & 0 & 0 & -4 & 0 & 0 \\
0 & 0 & 20 & 0 & 0 & 0 & 0 & 0 & 0 & 0 & -4 & 0 & 0 & 0 & -4 \\
-4 & 0 & 0 & 20 & 0 & 0 & 0 & -4 & 0 & 0 & 0 & 0 & 0 & 0 & 0 \\
0 & -4 & 0 & 0 & 20 & 0 & 0 & 0 & 0 & 0 & 0 & 0 & -4 & 0 & 0 \\
0 & 0 & 0 & 0 & 0 & 20 & 0 & 0 & 0 & -4 & 0 & 0 & 0 & -4 & 0 \\
0 & 0 & -4 & -24 & 24 & 28 & 72 & -12 & 36 & 16 & 8 & -36 & 12 & 16 & 8 \\
-4 & 0 & 0 & -4 & 0 & 0 & 0 & 20 & 0 & 0 & 0 & 0 & 0 & 0 & 0 \\
0 & -4 & 0 & -12 & 8 & 16 & 36 & -24 & 72 & 28 & 24 & -36 & 8 & 16 & 12 \\
0 & 0 & 0 & 0 & 0 & -4 & 0 & 0 & 0 & 20 & 0 & 0 & 0 & -4 & 0 \\
0 & 0 & -4 & 0 & 0 & 0 & 0 & 0 & 0 & 0 & 20 & 0 & 0 & 0 & -4 \\
-4 & 0 & 0 & 8 & -12 & -16 & -36 & 8 & -36 & -16 & -12 & 72 & -24 & -28 & -24 \\
0 & -4 & 0 & 0 & -4 & 0 & 0 & 0 & 0 & 0 & 0 & 0 & 20 & 0 & 0 \\
0 & 0 & 0 & 0 & 0 & -4 & 0 & 0 & 0 & -4 & 0 & 0 & 0 & 20 & 0 \\
0 & 0 & -4 & 0 & 0 & 0 & 0 & 0 & 0 & 0 & -4 & 0 & 0 & 0 & 20
\end{bmatrix}.$$

Finally, the matrix A_v is easily computed when we recall that the proxy field of the lowest order Whitney 3-form w^v is $\star w^v = 1/|v|$, so we only have to integrate barycentric functions

over the small tetrahedra. A_v and its inverse are

$$A_v = \frac{1}{64}\begin{bmatrix} 5 & 1 & 1 & 1 \\ 1 & 5 & 1 & 1 \\ 1 & 1 & 5 & 1 \\ 1 & 1 & 1 & 5 \end{bmatrix}, \quad A_v^{-1} = \begin{bmatrix} 14 & -2 & -2 & -2 \\ -2 & 14 & -2 & -2 \\ -2 & -2 & 14 & -2 \\ -2 & -2 & -2 & 14 \end{bmatrix}.$$

Approximating a p-form ω is similar as in lower dimensions. The approximation can be expressed as $\sum_s \alpha_s w^s$, where the sum is over small p-simplices and the coefficients α_s are determined as follows. Let v be any volume containing s and x the vector consisting of the integrals of ω over the small simplices of v. Then α_s is the dot product of x and the ith row of A^{-1}, where i is the index of s in v. The well-definedness of α_s is again seen from the matrices A^{-1} that we computed above: α_s does not depend on the choice of v.

Like before, at any point q, the only basis functions w^s that can be nonzero are those whose small simplex s is contained in a volume containing q. In practice the approximation of a p-form ω is not expressed in terms of the basis functions but can be evaluated at q using the following algorithms.

Algorithm 6 Approximating 0-forms in three dimensions.

1. Find the volume v containing q.
2. Compute the coefficient vector $a = (a_1, \ldots, a_{10})^T = A_n^{-1}x$, where $x = (x_1, \ldots, x_{10})^T$ contains the values of ω at the small nodes of v.
3. The approximation is $a_1 w^1(q) + \ldots + a_{10} w^{10}(q)$, where the forms w^i correspond to the small nodes of v.

Algorithm 7 Approximating 1-forms in three dimensions.

1. Find the volume v containing q.
2. Compute the coefficient vector $a = (a_1, \ldots, a_{20})^T = A_e^{-1}x$, where $x = (x_1, \ldots, x_{20})^T$ contains the integrals of ω over the small edges of v.
3. The approximation is $a_1 w^1(q) + \ldots + a_{20} w^{20}(q)$, where the forms w^i correspond to the small edges of v.

Algorithm 8 Approximating 2-forms in three dimensions.

1. Find the volume v containing q.
2. Compute the coefficient vector $a = (a_1, \ldots, a_{15})^T = A_f^{-1}x$, where $x = (x_1, \ldots, x_{15})^T$ contains the integrals of ω over the small facets of v.
3. The approximation is $a_1 w^1(q) + \ldots + a_{15} w^{15}(q)$, where the forms w^i correspond to the small facets of v.

Algorithm 9 Approximating 3-forms in three dimensions.

1. Find the volume v containing q.
2. Compute the coefficient vector $a = (a_1, \ldots, a_4)^T = A_v^{-1}x$, where $x = (x_1, \ldots, x_4)^T$ contains the integrals of ω over the small volumes of v.
3. The approximation is $a_1 w^1(q) + \ldots + a_4 w^4(q)$, where the forms w^i correspond to the small volumes of v.

As one may have noticed, the coefficient vector a in the preceding algorithms only depends on the volume v containing q but not directly on the point q. The approximation $\sum_i a_i w^i$ can actually be written as a sum of products of two barycentric functions and vectors that only depend on the volume of q. For example, in the case of 1-forms we have that

$$\begin{aligned} &a_1 w^1 + \ldots + a_{20} w^{20} = a_1 \lambda_m (\lambda_m \nabla \lambda_n - \lambda_n \nabla \lambda_m) + \ldots + a_{20} \lambda_k (\lambda_l \nabla \lambda_k - \lambda_k \nabla \lambda_l) \\ &= \lambda_m \lambda_m X_1 + \lambda_m \lambda_n X_2 + \lambda_m \lambda_l X_3 + \lambda_m \lambda_k X_4 + \lambda_n \lambda_n X_5 \\ &+ \lambda_n \lambda_l X_6 + \lambda_n \lambda_k X_7 + \lambda_l \lambda_l X_8 + \lambda_l \lambda_k X_9 + \lambda_k \lambda_k X_{10}, \end{aligned}$$

for some vectors X_i, where for example $X_1 = a_1 \nabla \lambda_n - a_2 \nabla \lambda_l + a_3 \nabla \lambda_k$. The vectors X_i stay the same in each volume, not depending on the point within that volume, and only need be computed once. This leads to significant computational savings when we wish to evaluate the approximation multiple times per volume. The same idea can also be used in the two-dimensional case with 1-forms.

For simplicity, we have thus far assumed that the small simplices that are discarded have the same indices in each tetrahedron. It's important to note that this is not necessary, and with small edges it actually can not be achieved. When we omit one small edge per facet in

each tetrahedron, we should ensure that the choice is consistent and doesn't depend on which side of the facet we are looking. In other words, the small edges that are dropped cannot be chosen in each tetrahedron independently of others.

But, this is not a problem, just something that we have to take into account. For each facet, there are three small edges to choose from — one of them must be omitted. Different choices lead to different matrices A, but the coefficients of other small edges than these three are not affected. In code, we check which of the three small edges is omitted, and compute the coefficients of the other two accordingly.

We don't provide examples similar to those in Sections 5.1 and 5.2 here, since the forms are more difficult to visualise in three dimensions and the idea should already be clear. However, we will continue with the three-dimensional case in the next section, where the model problem of Chapter 4 is solved using discrete exterior calculus with second order Whitney forms.

5.4 Second order approximations in discrete exterior calculus

Now we have practical algorithms for approximating differential p-forms in W_2^p, the space of second order Whitney forms. Next we show how second order Whitney forms are used in discrete exterior calculus. This is done by considering the model problem of Chapter 4. Recall that if a simplicial mesh is used, the solution method we gave in Chapter 4 corresponds to approximating the forms e and b with lowest order Whitney forms, i.e. in the spaces W^1 and W^2. We wish to modify the solution method so that the forms would be approximated in W_2^1 and W_2^2.

The idea is simple: we start with a simplicial mesh, refine the mesh such that the refined mesh contains all the small simplices, and solve the problem on the refined mesh, using the same method as in Chapter 4. The solution obtained is a cochain vector consisting of the integrals over the cells of the refined mesh. Since every small simplex is contained in the refined mesh, we know the integrals over the small simplices, and the solution can thus be expressed in W_2^p.

We must keep track of the small simplices of each tetrahedron in the old mesh. The linear dependency of the forms is dealt with as explained in Section 5.3: when the solution is evaluated, we omit one small edge and one small facet for each facet and tetrahedron in the old mesh (respectively). Note that this only affects the interpolation procedure; the solution method presented in Chapter 4 can be applied without any modifications. We just have to use it on the mesh that contains the small simplices.

The mesh may be refined in different ways, as long as the small simplices are contained in the refined mesh. Since the small tetrahedra of a tetrahedron v don't pave v, there will inevitably be other cells as well, and some of those might not even be simplices (recall Figure 4, left). This does not matter: as long as we know the integrals over the small simplices, they determine the corresponding element in W_2^p. The hole in Figure 4 can even be divided into smaller cells, and if it's divided into four tetrahedra, the refined mesh becomes simplicial as well.

Our solutions $e \in W_2^1$ and $b \in W_2^2$ can be evaluated at any point using the algorithms presented in Section 5.3, and the same ideas can be used to increase the efficiency of the evaluations when they are done multiple times in the same tetrahedron. Although it is not practical to write the solution in terms of the basis functions, from a theoretical point of view it is important that we could do so. This is because now the continuity properties of the solution are attained: tangential continuity for $e \in W_2^1$ and normal continuity for $b \in W_2^2$. The forms h, d, and j that are discretised on the dual mesh are not Whitney forms but can be expressed using the constitutive relations (4.3), (4.4), and (4.5) as $d = \varepsilon \star e$, $h = \frac{1}{\mu} \star b$, and $j = \sigma \star e$.

To test the method explained above, we consider the model problem of Chapter 4 with constant material parameters $\varepsilon = 2$, $\mu = 1$, and $\sigma = 1$. The domain D is a rhombic dodecahedron whose vertices contain $(\pm 1, 0, 0)^T$, $(0, \pm 1, 0)^T$, and $(0, 0, \pm 1)^T$ (see Figure 17). This domain suits well for testing second order Whitney forms since it's simple to build and refine a simplicial mesh in D. The boundary condition is given by

$$\vec{E}(x,y,z,t) = (0, \mathrm{Re}(e^{iwt-ikx}), \mathrm{Re}(-ie^{iwt-ikx}))^T = (0, \cos(wt-kx), \sin(wt-kx))^T,$$

with $k = w = 2\pi$. The initial values inside the domain are zero. Wave propagation is tracked forward in time by updating the values of **e** and **b** as explained in Chapter 4, but the values

of **e** on the boundary are given by the boundary condition.

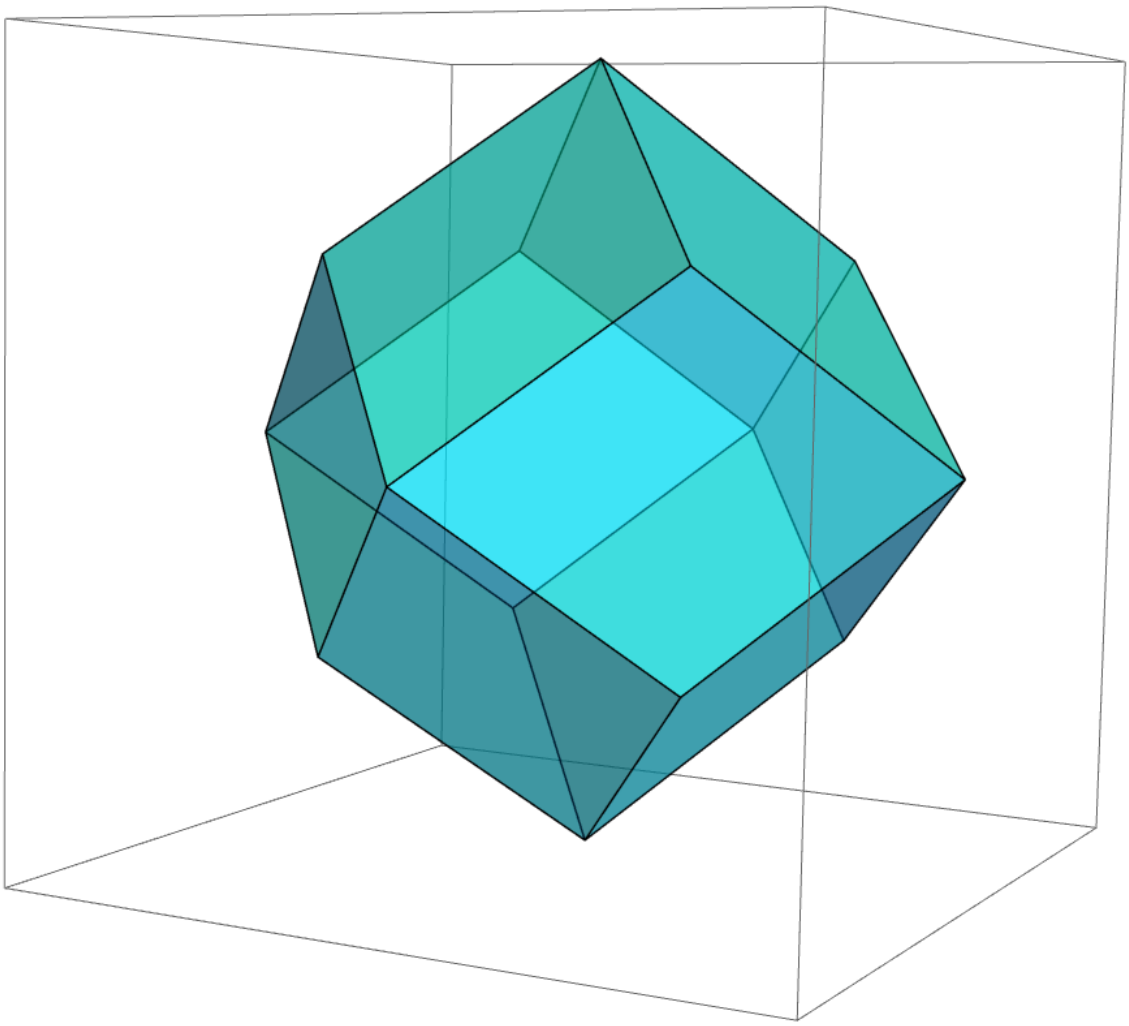

Figure 17. The domain used is a rhombic dodecahedron. The bounding box in the figure is the cube $[-1,1]^3$.

This problem is time-harmonic, and the steady-state solution has a time-harmonic expression as complex numbers. We express the real-valued field $\vec{E}(x,y,z,t)$ using a complex-valued field $\hat{\vec{E}}(x,y,z)$ without the time variable. The value of $\vec{E}$ at time instance t is then given by

$$\vec{E}(t) = \mathrm{Re}(\hat{\vec{E}}e^{iwt}). \tag{5.1}$$

We also have the complex-valued cochain vector $\hat{\mathbf{e}}$ which represents the integrals of $\hat{\vec{E}}$ over the edges of the mesh. Similarly, $\vec{B}$ and $\mathbf{b}$ are expressed without the time variable as $\hat{\vec{B}}$ and $\hat{\mathbf{b}}$.

Time integration is continued forward in time until a steady state has been reached and the solution is approximately time-harmonic. The resulting complex-valued cochain vectors can then be interpolated using complex-valued Whitney forms. This is done by simply interpolating real and imaginary parts separately. The value of the interpolated solution at time instance t is then given as in (5.1).

The simulation is done on six simplicial meshes with grains 2^{-j} for $j = 1, \ldots, 6$. This corresponds to refining the initial mesh five times, mesh j containing the small simplices of mesh $j-1$. The meshes have regular BCC structures; see Räbinä (2014) for the definition. When the mesh is refined, the hole in the left of Figure 4 is divided into four tetrahedra, so the number of tetrahedra is multiplied by eight. The initial mesh ($j = 1$) has 192 tetrahedra, and the mesh grain 2^{-j} here means the length of the longest edge of the tetrahedra.

To study the convergence, we examined the difference of the solutions $\hat{\vec{E}}_{j+1}$ and $\hat{\vec{E}}_j$ (and $\hat{\vec{B}}_{j+1}$ and $\hat{\vec{B}}_j$) yielded when interpolating the complex-valued cochain vectors on meshes $j+1$ and j. We estimated the L^2 norm of the difference numerically using a quadrature rule with five points per tetrahedron (Yu 1984; Keast 1986). For comparison this was done first with lowest order Whitney forms and then with second order Whitney forms. The results are displayed in Table 6.

L^2 norm of the difference $\hat{\vec{E}}_{j+1} - \hat{\vec{E}}_j$				
j	2	3	4	5
Lowest order Whitney 1-forms	2.09902	0.84525	0.39412	0.19369
Second order Whitney 1-forms	1.91274	0.48106	0.12333	0.032869

L^2 norm of the difference $\hat{\vec{B}}_{j+1} - \hat{\vec{B}}_j$				
j	2	3	4	5
Lowest order Whitney 2-forms	3.67633	1.48184	0.66862	0.31981
Second order Whitney 2-forms	3.58869	1.14689	0.41462	0.17194

Table 6. L^2 norm of the difference of the interpolated solutions on consecutive meshes.

The results indicate faster convergence with second order Whitney forms, especially in the case of electric fields (see also Figure 18). With magnetic fluxes the advantage is not so

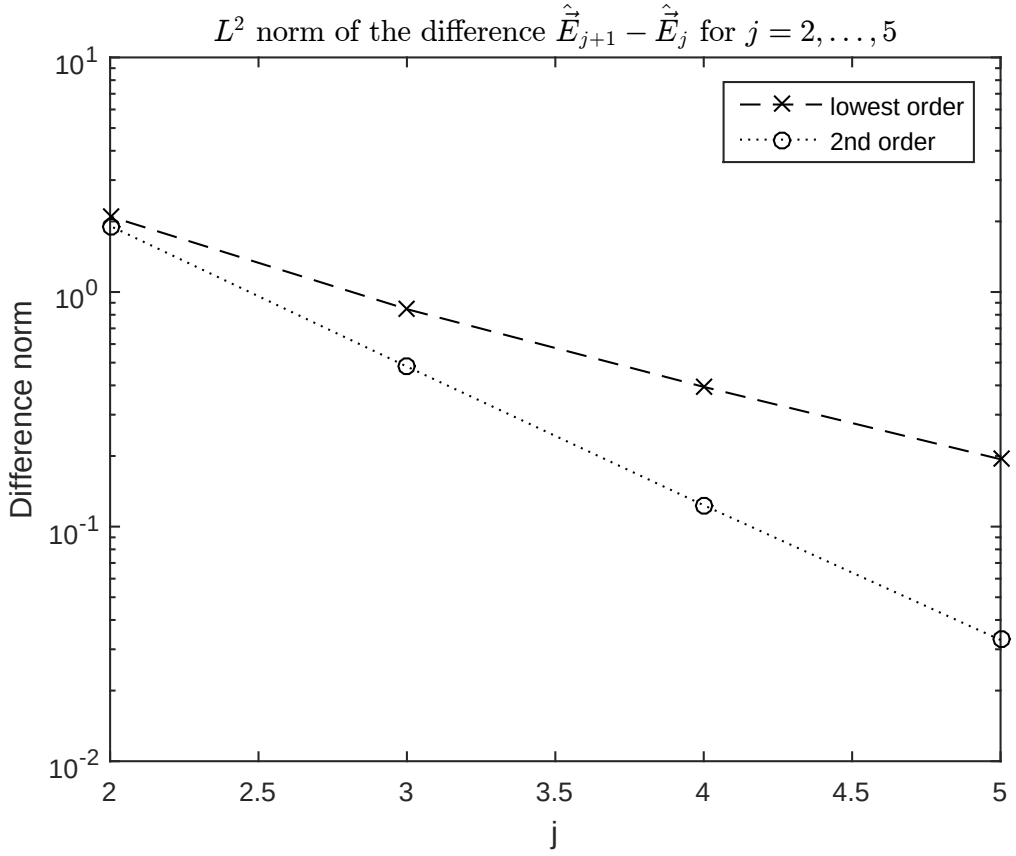

Figure 18. Visualisation of the results for electric fields displayed in Table 6.

clear, and the difference is considerable even between the last two meshes. This suggests that the error made when approximating the Hodge star operator during time integration is dominantly affecting the results. To verify this, we computed the average difference of the cochain vectors $\hat{\mathbf{e}}_{j+1}$ and $\hat{\mathbf{e}}_j$ over the edges of mesh j. The values of $\hat{\mathbf{e}}_{j+1}$ are obtained by summing the values on corresponding small edges of mesh $j+1$. The modulus of the difference on each edge was normalised by dividing by the edge length, and then we took the average over all edges. Similar computations were done for $\hat{\mathbf{b}}_{j+1}$ and $\hat{\mathbf{b}}_j$ on the facets of mesh j. The results are shown in Table 7.

j	2	3	4	5
Average difference between $\hat{\mathbf{e}}_{j+1}$ and $\hat{\mathbf{e}}_j$	0.42703	0.11598	0.030000	0.0076605
Average difference between $\hat{\mathbf{b}}_{j+1}$ and $\hat{\mathbf{b}}_j$	0.97487	0.33809	0.13011	0.055829

Table 7. The average difference of the discrete solutions on consecutive meshes.

The results confirm that the magnetic fluxes already contain error before the interpolation stage. The total error consists of the Hodge approximation error made during time integration and the interpolation error. The Hodge approximation error cannot be affected in the interpolation stage, but the results suggest that the interpolation error can be reduced significantly with the use of second order Whitney forms. It is a topic for future research whether higher order Whitney forms could also be used to improve the Hodge approximation; this would of course require changes in the time integration procedure.

In addition to the convergence properties, we must also consider computational costs when assessing whether second order Whitney forms are worth using. Time integration is done using the same method but on the refined mesh. We used lowest order Whitney forms of the refined mesh when the results were compared, so the computational costs during time integration were unchanged.

One might expect that interpolating with second order Whitney forms would be computationally more expensive than with lowest order Whitney forms, since the degrees of freedom must be computed as linear combinations of values on small simplices. However, the matrices A^{-1} which determine the coefficients are rather sparse, and with second order Whitney forms we can take advantage of the parts of the solution that stay the same in each volume, as explained earlier. When the solution is evaluated multiple times per big tetrahedron, these parts only need be computed once. The same strategy can be used with lowest order Whitney forms, but then the unchanged parts only stay the same in each small tetrahedron, so the advantage is not equally great.

Based on our observations, it seems that interpolating with lowest order Whitney forms is somewhat faster when the number of evaluations is low, and interpolating with second order Whitney forms is slightly faster when the solution is evaluated multiple times per tetrahedron. The difference is not significant though, and in any case, the computation time used during interpolation is unimportant in comparison to that used in time integration.

Hence, the use of second order Whitney forms seems worthwhile, as long as we have a simplicial mesh and its refinement to begin with. However, the requirement that the initial mesh be simplicial is restrictive in discrete exterior calculus, and it would be desirable to

have differential forms that correspond to cochains defined on the space of more general cells, i.e. counterparts of Whitney forms on nonsimplicial meshes. This subject has been discussed in the literature e.g. by Gradinaru and Hiptmair (1999) and Bossavit (2005, 2010), and it seems to be a fitting topic for future research, especially in the higher order case.

6 Conclusions

Whitney forms are finite elements for differential forms on simplicial meshes. In this thesis, we have defined higher order Whitney forms and shown how they can be used to approximate differential forms in a finite basis. The construction of higher order Whitney spaces is based on the so-called small simplices, which are images of the mesh simplices through homothetic transformations. The initial mesh is refined such that the small simplices are contained in the refined mesh.

Like each p-simplex of the initial mesh is associated with a lowest order Whitney p-form, to each small p-simplex corresponds a higher order Whitney p-form. These are not linearly independent, but some of them can be discarded to obtain a basis for the higher order Whitney space W_k^p. The forms spanning W_k^p are products between a Whitney p-form of lowest order and continuous barycentric functions, so the elements in W_k^p possess the same conformity properties as lowest order Whitney p-forms.

When differential forms are approximated with lowest order Whitney forms, the degrees of freedom are the integrals over the mesh simplices. The approximation is the Whitney form whose integrals match with those of the initial form over the mesh simplices. In the higher order case, the degrees of freedom are linear combinations of the integrals over small simplices. For this we omit the small simplices whose corresponding forms were discarded when choosing a basis. The degrees of freedom are then determined such that the approximation has the same integrals as the initial form over the rest of the small simplices. When the basis is fixed, this can be done in a consistent way, and the degrees of freedom corresponding to small simplices that belong to multiple mesh elements do not depend on which side of the inter-element face we are looking.

In the practical part of the thesis we considered the implementation of second order Whitney forms. We computed the matrices which determine the degrees of freedom and provided algorithms for approximating differential forms in one-, two-, and three-dimensional cases. The algorithms were demonstrated with illustrating examples, and the convergence properties were studied by comparing the L^2 norm of the approximation error to the lowest order

case with different mesh grains. The results indicate a significantly better convergence rate with second order forms.

The main research problem of the thesis was how higher order Whitney forms can be used in discrete exterior calculus when solving partial differential equations expressed in terms of differential forms. With our construction of the higher order Whitney spaces, this can be done with very small adaptations to the method. We refine a simplicial mesh such that the small simplices are contained in the refined mesh, and then the same time integration procedure can be used on the refined mesh without any modifications. The resulting discrete solution includes the integrals over the small simplices, and the solution can thus be expressed in the chosen basis of the higher order Whitney space.

The method we developed was tested by solving a model problem based on Maxwell's equations. We compared the convergence in L^2 norm with the lowest order case. The results indicate that the interpolation error can be reduced significantly by using second order Whitney forms, while the computational costs stay unchanged. This requires a simplicial mesh and its refinement that contains the small simplices. The requirement that the initial mesh be simplicial is restrictive in discrete exterior calculus, and in future research we aim to study what kind of finite elements for differential forms can be associated with more general cells, i.e. what are the counterparts of Whitney forms on nonsimplicial meshes.

Bibliography

Abraham, R., J.E. Marsden, and T. Ratiu. 2012. *Manifolds, Tensor Analysis, and Applications.* Applied Mathematical Sciences. Springer New York.

Ainsworth, Mark, and Joe Coyle. 2003. "Hierarchic finite element bases on unstructured tetrahedral meshes". *International Journal for Numerical Methods in Engineering* 58 (14): 2103–2130.

Arnold, Douglas N., Richard S. Falk, and Ragnar Winther. 2006. "Finite element exterior calculus, homological techniques, and applications". *Acta Numerica* 15:1–155.

Bishop, R.L., and S.I. Goldberg. 1980. *Tensor Analysis on Manifolds.* Dover Books on Mathematics. Dover Publications.

Bonazzoli, Marcella, and Francesca Rapetti. 2017. "High-order finite elements in numerical electromagnetism: degrees of freedom and generators in duality". *Numerical Algorithms* 74 (1): 111–136.

Bonazzoli, Marcella, Francesca Rapetti, and Chiara Venturini. 2018. "Dispersion analysis of triangle-based Whitney element methods for electromagnetic wave propagation". *Applied Mathematics and Computation* 319:274–286.

Boothby, William M. 1986. *An introduction to differentiable manifolds and Riemannian geometry.* Academic Press.

Bossavit, Alain. 1988. "Whitney forms: a class of finite elements for three-dimensional computations in electromagnetism". *IEE Proceedings A - Physical Science, Measurement and Instrumentation, Management and Education - Reviews* 135 (8): 493–500.

———. 1998. *Computational electromagnetism: variational formulations, complementarity, edge elements.* Academic Press.

———. 2002. "Generating Whitney forms of polynomial degree one and higher". *IEEE Transactions on Magnetics* 38 (2): 341–344.

Bossavit, Alain. 2005. “Discretization of Electromagnetic Problems: The “Generalized Finite Differences” Approach”. *Handbook of Numerical Analysis* 13:105–197.

———. 2010. “A uniform rationale for Whitney forms on various supporting shapes”. *Mathematics and Computers in Simulation* 80 (8): 1567–1577.

Bossavit, Alain, and Lauri Kettunen. 1999. “Yee-like schemes on a tetrahedral mesh, with diagonal lumping”. *International Journal of Numerical Modelling: Electronic Networks, Devices and Fields* 12 (1-2): 129–142.

Christiansen, Snorre H., and Francesca Rapetti. 2016. “On high order finite element spaces of differential forms”. *Math. Comput.* 85:517–548.

Desbrun, M., A. N. Hirani, M. Leok, and J. E. Marsden. 2005. “Discrete Exterior Calculus”. *ArXiv Mathematics e-prints.*

Dodziuk, Jozef. 1976. “Finite-difference approach to the Hodge theory of harmonic forms”. *American Journal of Mathematics* 98 (1): 79–104.

Dunavant, D.A. 1985. “High degree efficient symmetrical Gaussian quadrature rules for the triangle”. *International journal for numerical methods in engineering* 21 (6): 1129–1148.

Gradinaru, Vasile, and Ralf Hiptmair. 1999. “Whitney elements on pyramids”. *Electronic Transactions on Numerical Analysis* 8:154–168.

Grady, Leo J., and Jonathan R. Polimeni. 2010. *Discrete calculus: Applied analysis on graphs for computational science.* Springer Science & Business Media.

Hatcher, A. 2002. *Algebraic Topology.* Cambridge University Press.

Hiptmair, Ralf. 2001. “Higher order Whitney forms”. *Progress in Electromagnetics Research* 32:271–299.

Keast, Patrick. 1986. “Moderate-degree tetrahedral quadrature formulas”. *Computer Methods in Applied Mechanics and Engineering* 55 (3): 339–348.

Kirby, Robert C., Anders Logg, Marie E. Rognes, and Andy R. Terrel. 2012. “Common and unusual finite elements”. In *Automated Solution of Differential Equations by the Finite Element Method,* 95–119. Springer.

Lee, John M. 2012. *Introduction to Smooth Manifolds.* 2. ed. Graduate Texts in Mathematics. Springer.

Maunder, C.R.F. 1996. *Algebraic Topology.* Dover Books on Mathematics. Dover Publications.

Munkres, J.R. 1991. *Analysis on manifolds.* Advanced Book Classics. Addison-Wesley Publishing Company, Advanced Book Program.

Nédélec, Jean-Claude. 1980. "Mixed finite elements in $\mathbb{R}^3$". *Numerische Mathematik* 35 (3): 315–341.

———. 1986. "A new family of mixed finite elements in $\mathbb{R}^3$". *Numerische Mathematik* 50 (1): 57–81.

Räbinä, Jukka. 2014. "On a numerical solution of the Maxwell equations by discrete exterior calculus". *Jyväskylä studies in computing,* number 200.

Räbinä, Jukka, Lauri Kettunen, Sanna Mönkölä, and Tuomo Rossi. 2018. "Generalized wave propagation problems and discrete exterior calculus". *ESAIM: M2AN* 52 (3): 1195–1218.

Rapetti, Francesca. 2007. "High order edge elements on simplicial meshes". *ESAIM: M2AN* 41 (6): 1001–1020.

Rapetti, Francesca, and Alain Bossavit. 2007. "Geometrical localisation of the degrees of freedom for Whitney elements of higher order". *IET Science, Measurement & Technology* 1 (1): 63–66.

———. 2009. "Whitney Forms of Higher Degree". *SIAM Journal on Numerical Analysis* 47 (3): 2369–2386.

Spivak, M. 1999. *A Comprehensive Introduction to Differential Geometry.* 3. ed. Volume 1. Publish or Perish.

Whitney, H. 1957. *Geometric integration theory.* Princeton University Press.

Yee, Kane. 1966. "Numerical solution of initial boundary value problems involving Maxwell's equations in isotropic media". *IEEE Transactions on antennas and propagation* 14 (3): 302–307.

Yu, Jinyun. 1984. “Symmetric Gaussian quadrature formulae for tetrahedronal regions”. *Computer Methods in Applied Mechanics and Engineering* 43 (3): 349–353.